

# High Field Advanced MRI

## Uwe Eichhoff

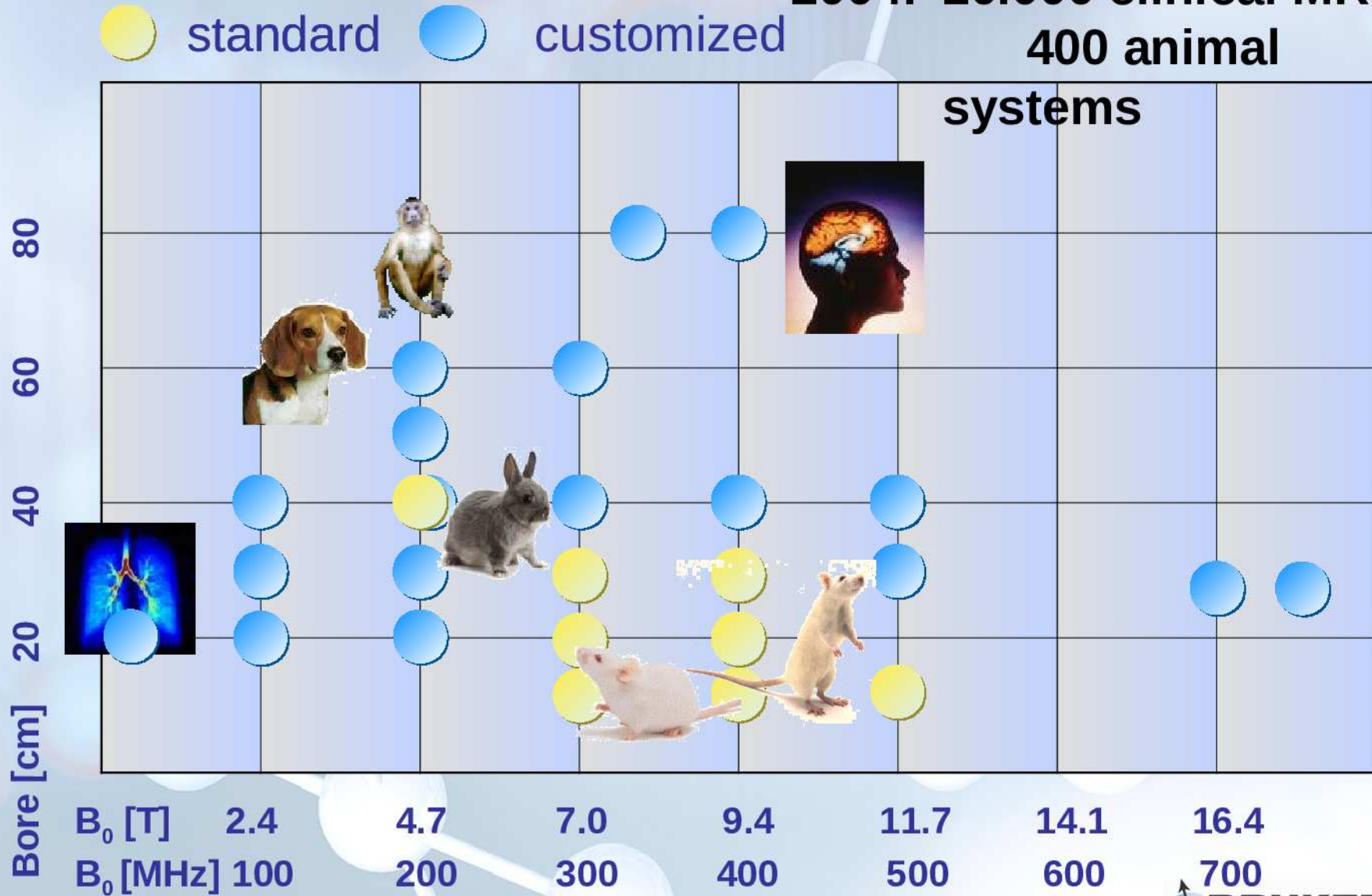
### Tallinn 2006



# Custom Solutions: Magnets



2004: 20.000 clinical MRI  
400 animal systems



# Highest Field Clinical MRI

**University of Illinois, Chicago**

9.4 Tesla, 80cm bore

# Highest Field for Animal Research MRI

**Max Planck Institute for Biocybernetics**

**Tübingen** 16.4 Tesla, 26cm bore

**CEA Paris projet Neurospin**

17.6 Tesla, 25cm bore

*9.4 T Head Scanner @ UIC*



# Cutting edge

MRI/MRS human head scanner

**9.4 Tesla**



**80 cm bore**



**University of Illinois,  
Chicago**



# 9.4 T Head Scanner @ UIC



## Magnet

- 9.4 Tesla 80 cm bore



## Head Gradient Coil:

- Asymmetric, clear bore access 36cm

## RF Coil

- $^{23}\text{Na}$  birdcage type resonator



## Gradient Amplifier

- Copley 281 with 700V/500A



## Shim Amplifier

- 12 channel, max. 10A



## Electronics

- Biospec® 4TX / 4 RX electronics
- ParaVision®
- TPI prototype implementation



# 9.4 T Head Scanner @ UIC



## First Results: Proc. ISMRM, 3103, 2006, feat. by A. Nauerth, Bruker

### Initial Experience with Sodium MRI of Phantoms and Human Brain at 9.4 Tesla

F. Damen<sup>1</sup>, S. Holdsworth<sup>2</sup>, I. Atkinson<sup>3</sup>, E. Boskamp<sup>4</sup>, T. Chabotiere<sup>4</sup>, A. Nauerth<sup>5</sup>, B. Li<sup>2</sup>, X. J. Zhou<sup>2</sup>, Z-P. Liang<sup>5</sup>, K. R. Thulborn<sup>1</sup>  
<sup>1</sup>Centre of MR Research, University of Illinois Medical Center, Chicago, IL, United States, <sup>2</sup>Centre for Magnetic Resonance, University of Queensland, Brisbane, Queensland, Australia, <sup>3</sup>Applied Science Laboratory GE Healthcare, Waukesha, WI, United States, <sup>4</sup>Bruker Biospin, Ratingen, Germany, <sup>5</sup>Beckman Institute, University of Illinois, Urbana, IL, United States

#### INTRODUCTION:

Our initial experience with the 9.4 Tesla scanner for human imaging has focused on sodium MR imaging with two-dimensional projection imaging (TPI) [1]. We have used phantoms to measure signal to noise improvements compared to 3T with resultant improvements in spatial resolution and specific absorption rates (SAR). The first human brain sodium images have been acquired within FDA guidelines for SAR with reduced acquisition times as would be expected compared to 3T.

#### METHODS:

The 9.4-Tesla magnet and head gradient set (GE Healthcare, UK) were custom built for human imaging (clear magnet bore diameter of 80cm, clear gradient bore access of 36cm from patient end of gradient housing) and interfaced to spectrometer electronics (Bruker Biospin, Germany) to provide a full imaging suite for proton and non-proton imaging including capabilities for SAR monitoring, and higher order shimming (14 channels, driven by power supplies from Resonance Research, Inc., MA). A modified birdcage volume RF coil (diameter 26cm) tuned to sodium frequency (105.9MHz) was used for all experiments. The resolution phantom was a sphere filled with 150mM sodium chloride but containing a line of rods of 4 different sizes (2.6, 19.1, 127, 6.4mm, respectively). The smallest rods were placed in two pairs separated by their diameter. This phantom was used to establish the experimental spatial resolution of the sodium images. Human imaging was performed on the only individual permitted to enter the magnet to obtain *in vivo* sodium concentrations (TSC). For comparison to 3T [2] calibration phantoms contained 30 and 90mM sodium chloride. Sodium T1 time was measured using a progressive saturation experiment analyzed as a semi-logarithmic plot of signal intensity against repetition rate (TR).

Sodium MR imaging was developed using the efficient TPI sequence using parameters that avoided T1 saturation by appropriate choice of TR and minimized T2 signal loss by using the shortest TE (TR = 120ms, TE = 0.41ms, flip angle = 90°, number of averages = 1, maximum gradient strength 4mT/m, resolution = 5x5x5mm<sup>3</sup>, number of projections for radial fractions of 0.4 and 1.0 = 2070 and 5100, respectively, giving total acquisition times = 4.14 and 10.2 minutes for radial fractions of 0.4 and 1, respectively) [1]. Sodium images were reconstructed and quantified as previously described [1,2,3].

#### RESULTS:

Figure 1 shows the sodium images of the phantom for radial fractions of 1.0 and 0.4 with corresponding SNR of 20.2 and 18.6 and total acquisition times of 10.2 and 4.1 minutes, respectively. T1 of sodium in free solution was 45ms. Circulation of signal intensity shows the B1 variation across the field of view. Figure 2 shows representative partitions from the human brain sodium images in three planes with a SNR of 25. Quantitative tissue sodium concentrations of brain parenchyma vary between 30 and 36mM, which are similar to published results from longer acquisitions at 3T [2]. SAR images set by the FDA guidelines were not closely approached (<25%) during these *in vivo* acquisitions despite the short TR. Field homogeneity of less than 0.4ppm over the human head was achieved by shimming on the sodium signal.

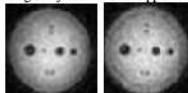


Figure 1. One partition from 3D Na TPI dataset acquired with radial fraction of 1.0 (left) and 0.4 (right). The separation of the small rods is evident.

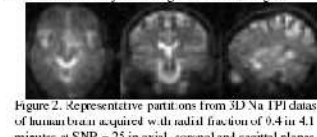
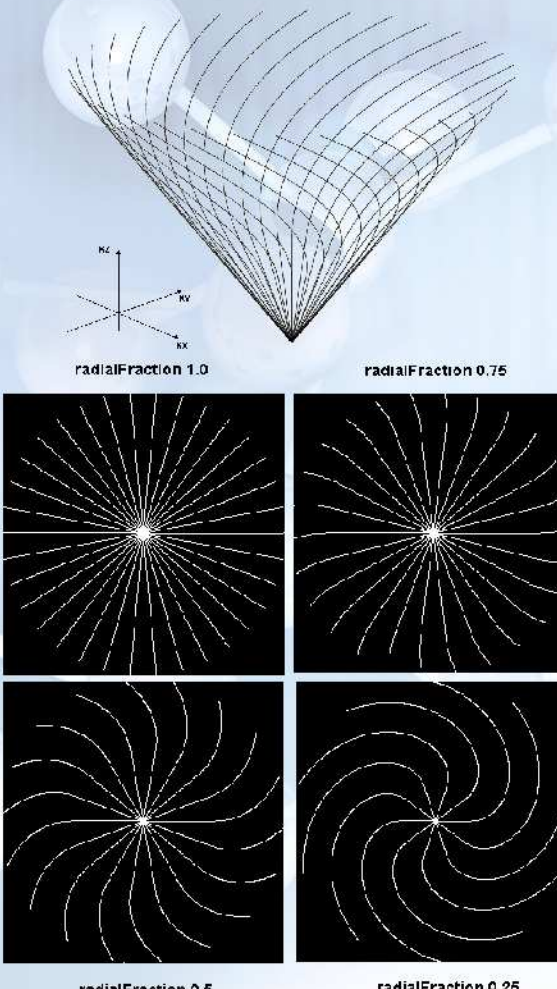


Figure 2. Representative partitions from 3D Na TPI dataset of human brain acquired with radial fraction of 0.4 in 4.1 minutes at SNR = 25 in axial, coronal and sagittal planes.

#### DISCUSSION:

Sodium imaging has been achieved on this 9.4T scanner designed for human imaging with acceptable spatial resolution for quantification achieved previously at 3T but at shorter acquisition times. Homogeneity and SAR are not limitations. REFERENCE: 1. Boada HE, Christensen JS, Gillen JS, Tauborn K. Magn Reson Med 1997;37:470-71.

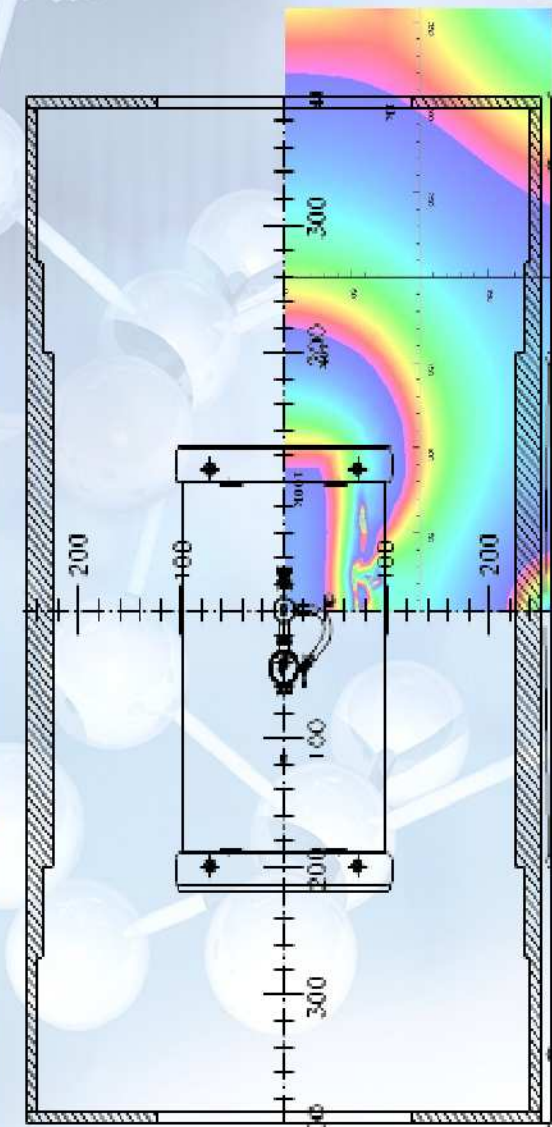
2. Thulborn KR, Gindin TS, Davis D, Erft P. Radiology 1999;139:26-34. 3. Jackson JL, Meyer CH, Nishimura DG, Macovski A. IEEE Trans Med Imaging 1991;10:473-478. Grant acknowledgement: P01-NS386760.

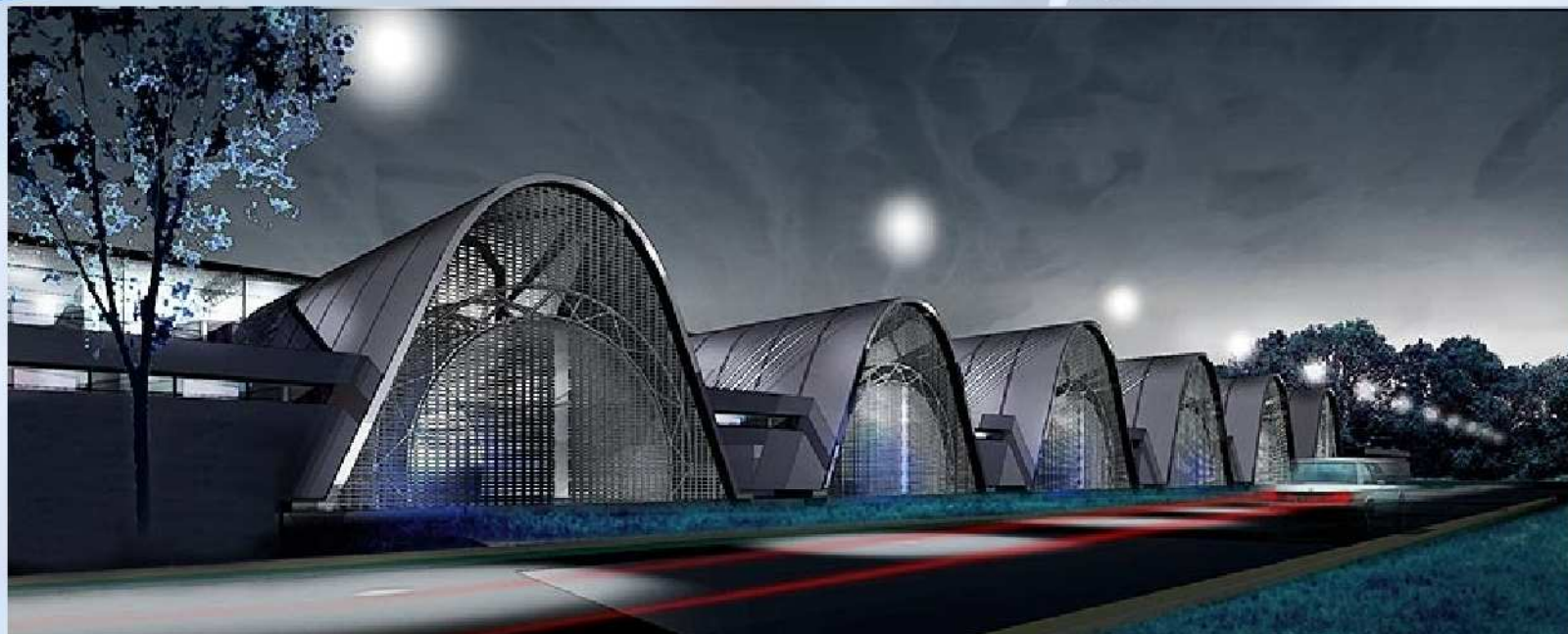


# BioSpec® 164/26 @ MPIfBC (Germany)

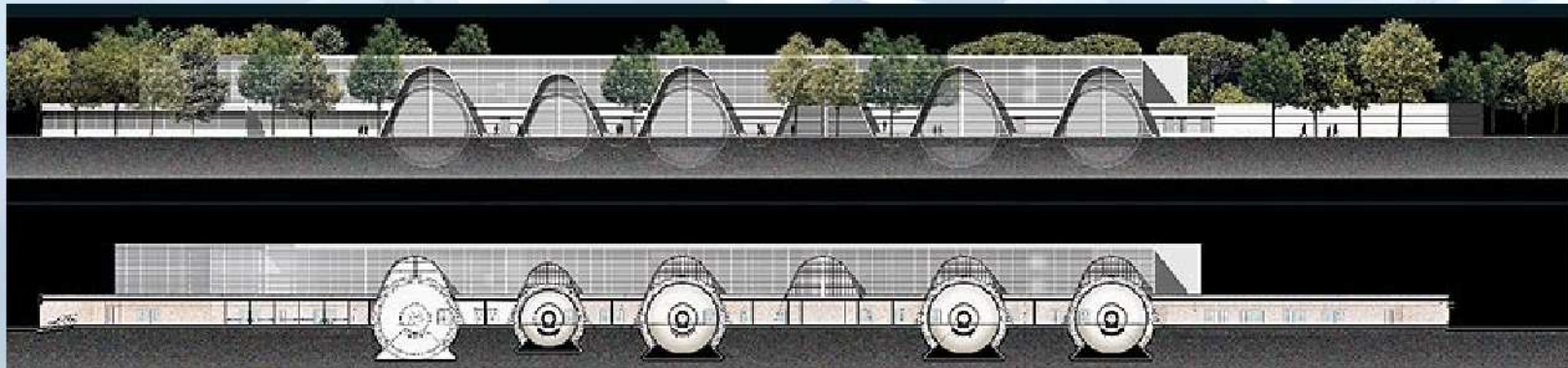


Kamil  
Ugurbil





## Projet NeuroSpin...



# Why High Field MRI ?



## Diffusion/Perfusion

## Functional MRI

## Diffusion Tensor MRI

## MR in vivo Spectroscopy

## Molecular Imaging



# new development

# wireless cardiac

# gating

# IntraGate: Wireless Cardiac Cine



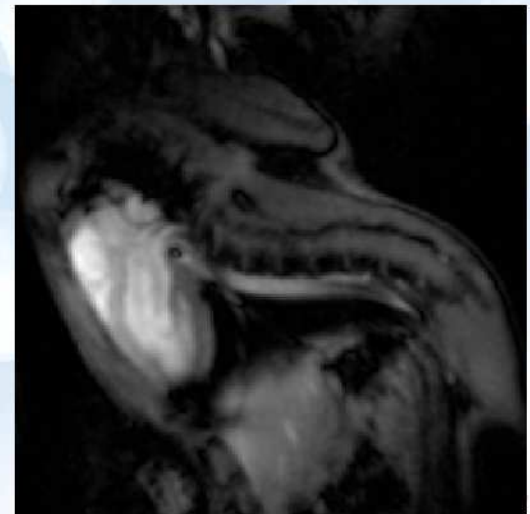
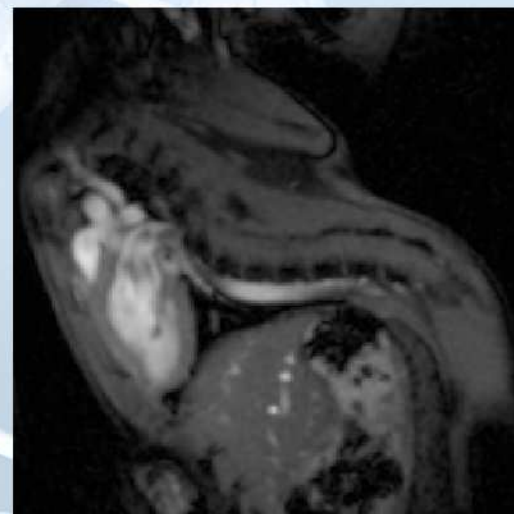
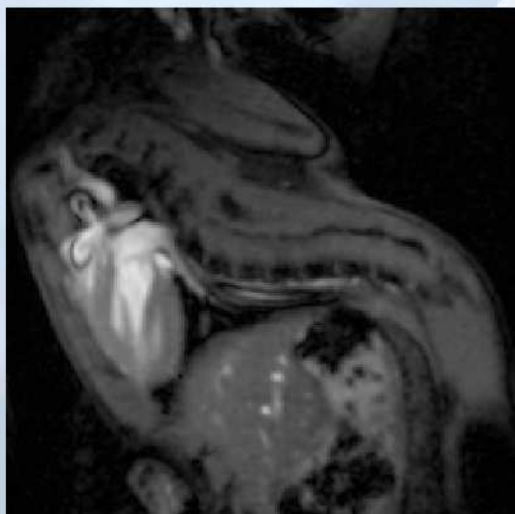
Cardiac Movie



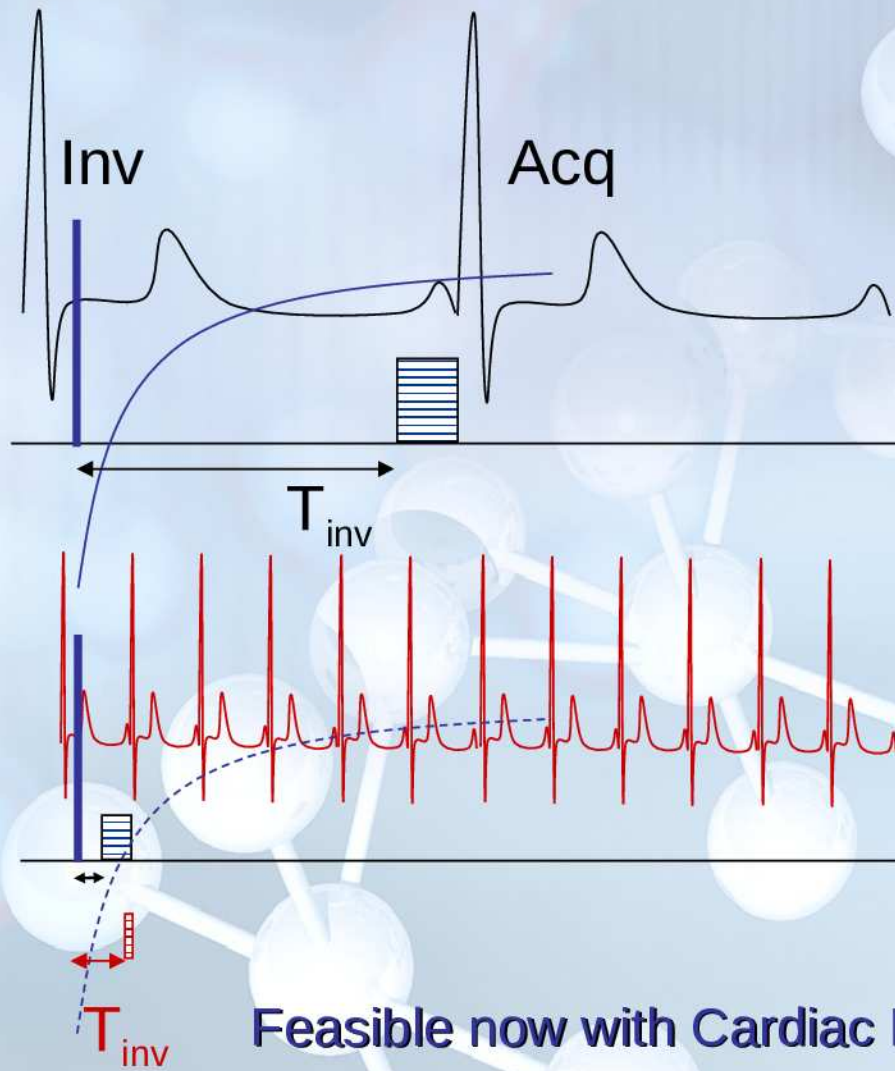
Respiration Movie



Cardiac & Respiration



# First-Pass Myocardial Perfusion



Rat Heart (*in vivo*)  
IR-FISP

CM after 10 s

Bolus: 0.04 mMol/kg

Magnevist® (CM)

TI: 100 ms

TR: 1.6 ms

TE: 0.7 ms

Acc Factor: 2

Matrix:  $64 \times 48$

FOV:  $(3 \times 2) \text{ cm}$

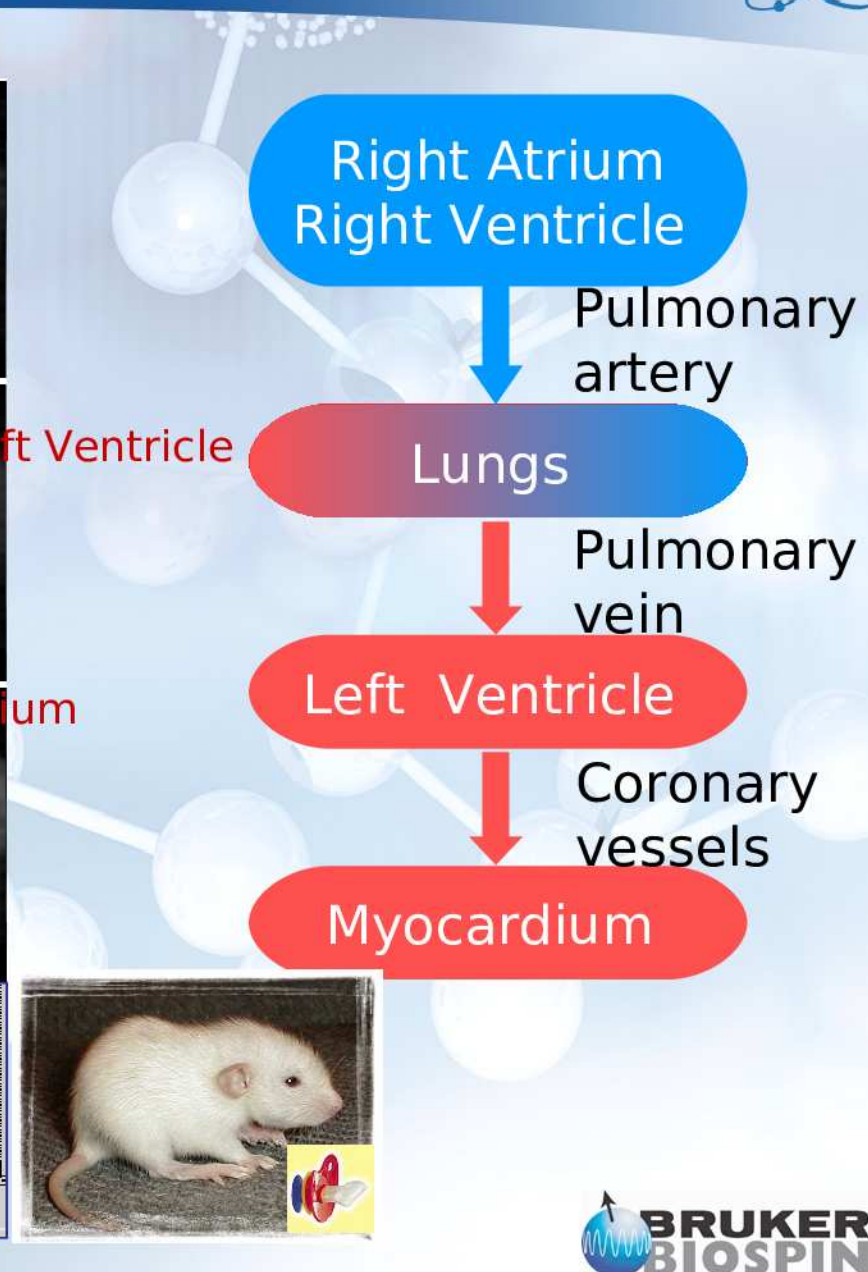
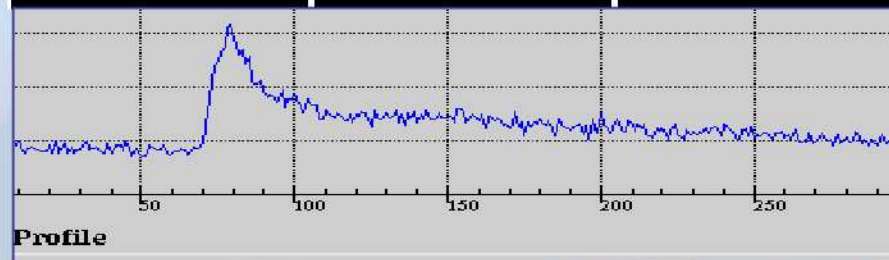
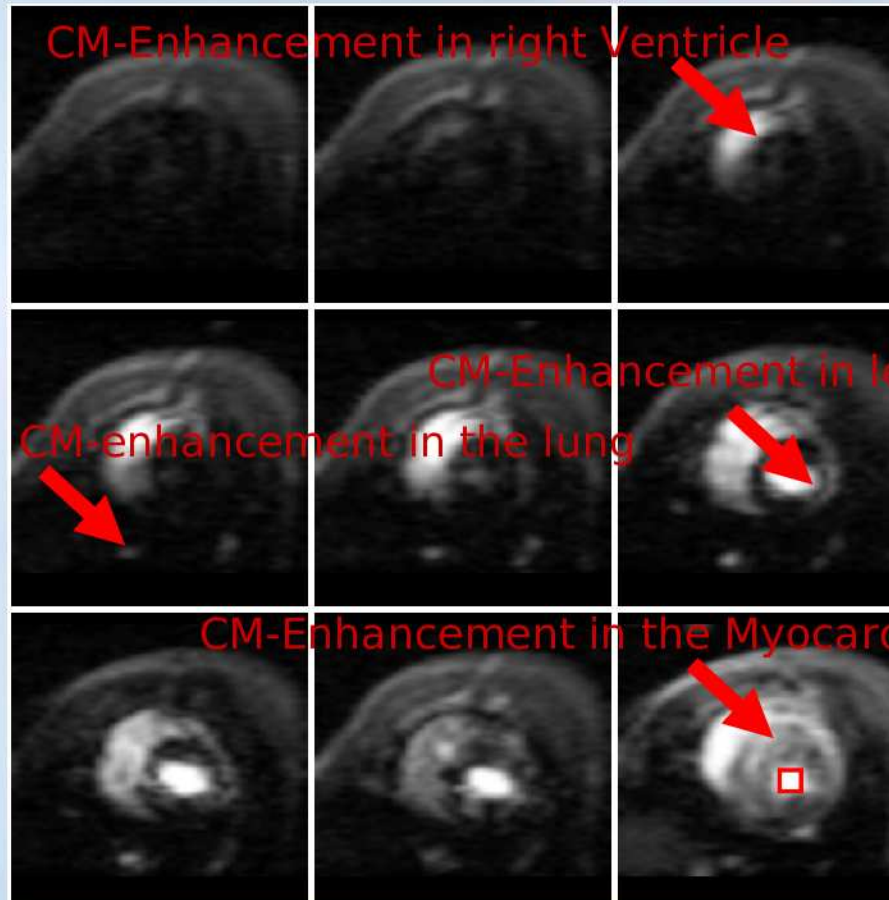
Total Scan Time: 152 ms

**1 Image per Heart Beat !**

300 Repetitions

Feasible now with Cardiac Phased Array Coil!

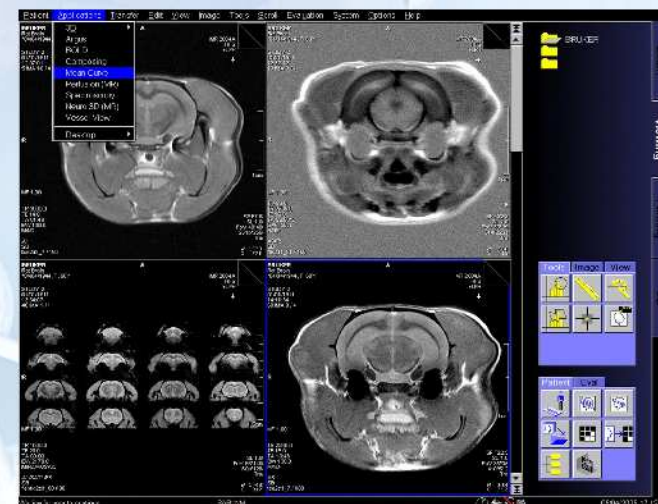
# First-Pass Myocardial Perfusion



# CLINSCAN

## Animal System compatible with Clinical Human Whole Body MRI

## A new animal MRI scanner from Bruker based on Siemens technology



# Components from Two Worlds



- **Bruker magnet technology**
  - High field 7T USR  
(ultra shielded refrigerated)
- **Bruker gradient and shim system**
  - actively shielded (> 99 % shielding)  
integrated gradient and shim system
- **Bruker animal handling and monitoring solutions**

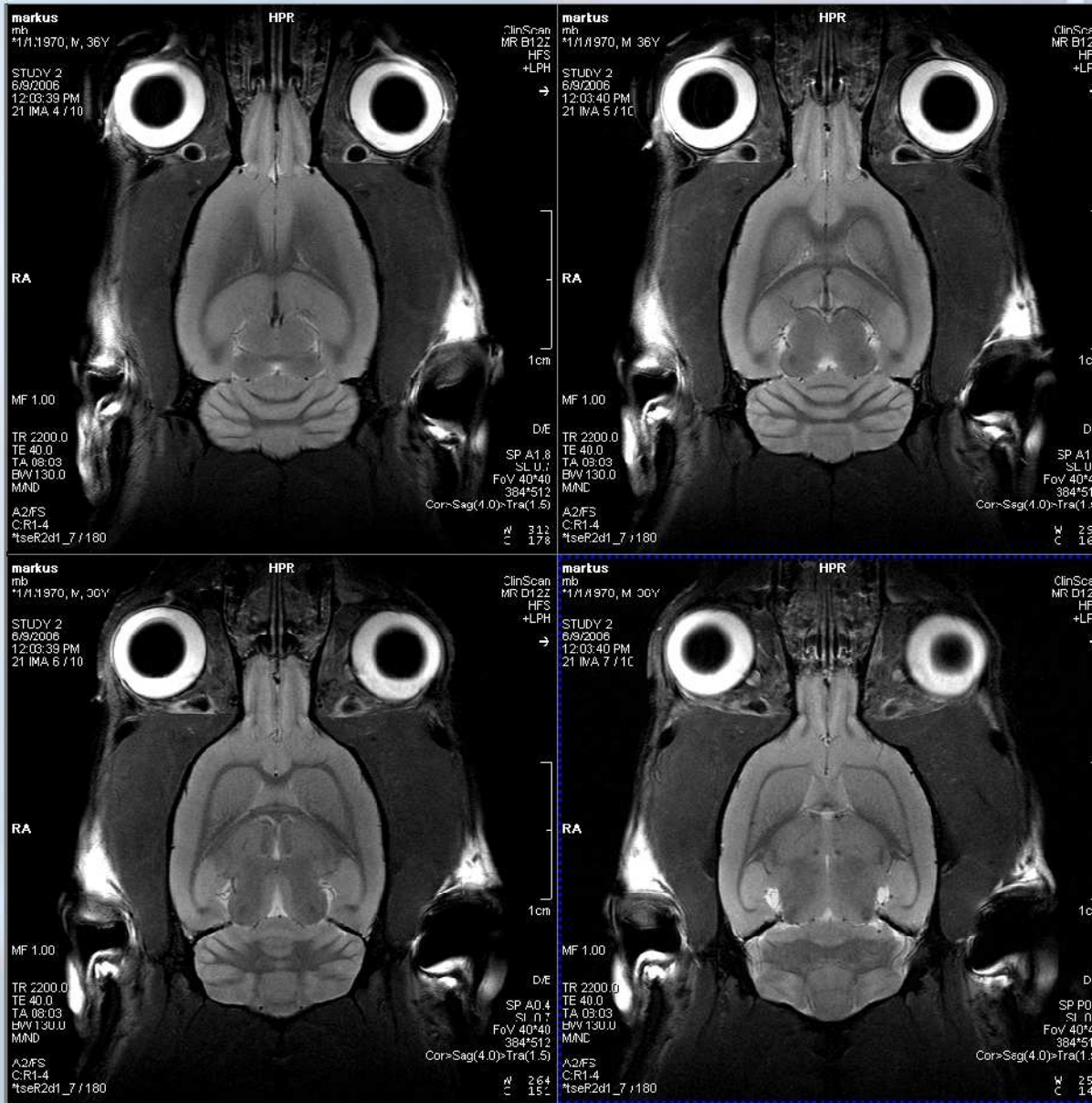


- **Siemens MAGNETOM Avanto User Interface**
- **Siemens Syngo**
- **Siemens small signal components and data chain**

SIEMENS



# High Resolution T2 Imaging



Rat brain  
 $78 \times 104 \mu\text{m}^2$   
in plane resolution

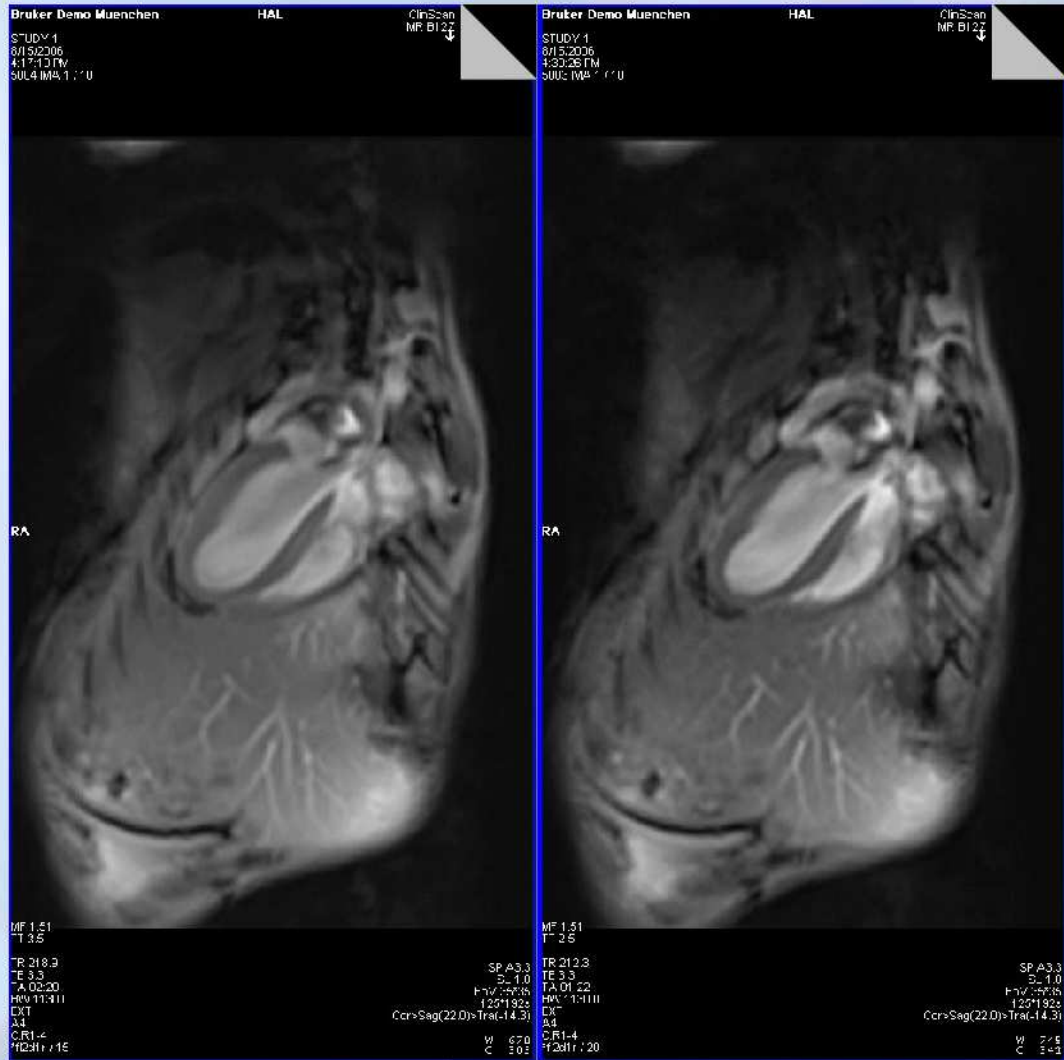
Turbo Spin Echo  
Imaging

2x2 Rat brain coil

FOV:  $40 \times 40 \text{ mm}^2$ ,  
matrix 384x512,  
TE/TR: 41/2000 ms



# Cine Cardiac Imaging: Grappa



FOV: 35x35 mm<sup>2</sup>, matrix 125x192  
TE/TR 3.3/7 ms

Mouse heart  
Cine FLASH Imaging  
ECG and respiratory  
gating  
7ms temporal  
resolution  
left: 2:20 min  
right: GRAPPA factor 2  
1:22 min

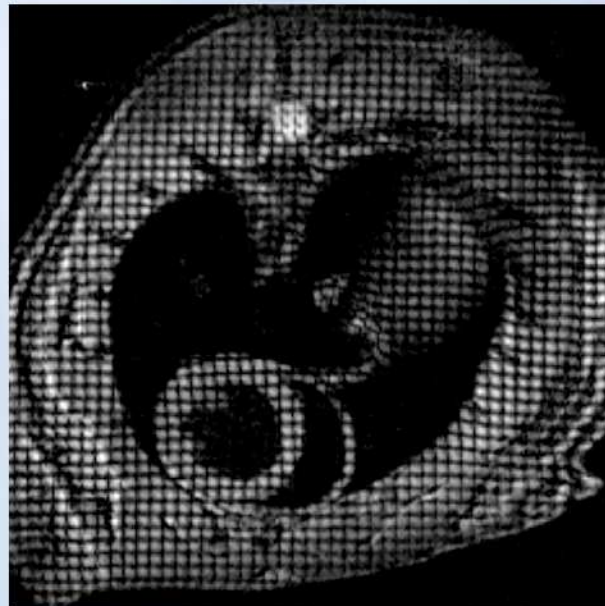


# BioSpec® 94/20: Black Blood+Tagging

rat heart (*in vivo*)

FLASH Black Blood + Tagging

Cardiac gated, Coil: 72 mm linear Res.

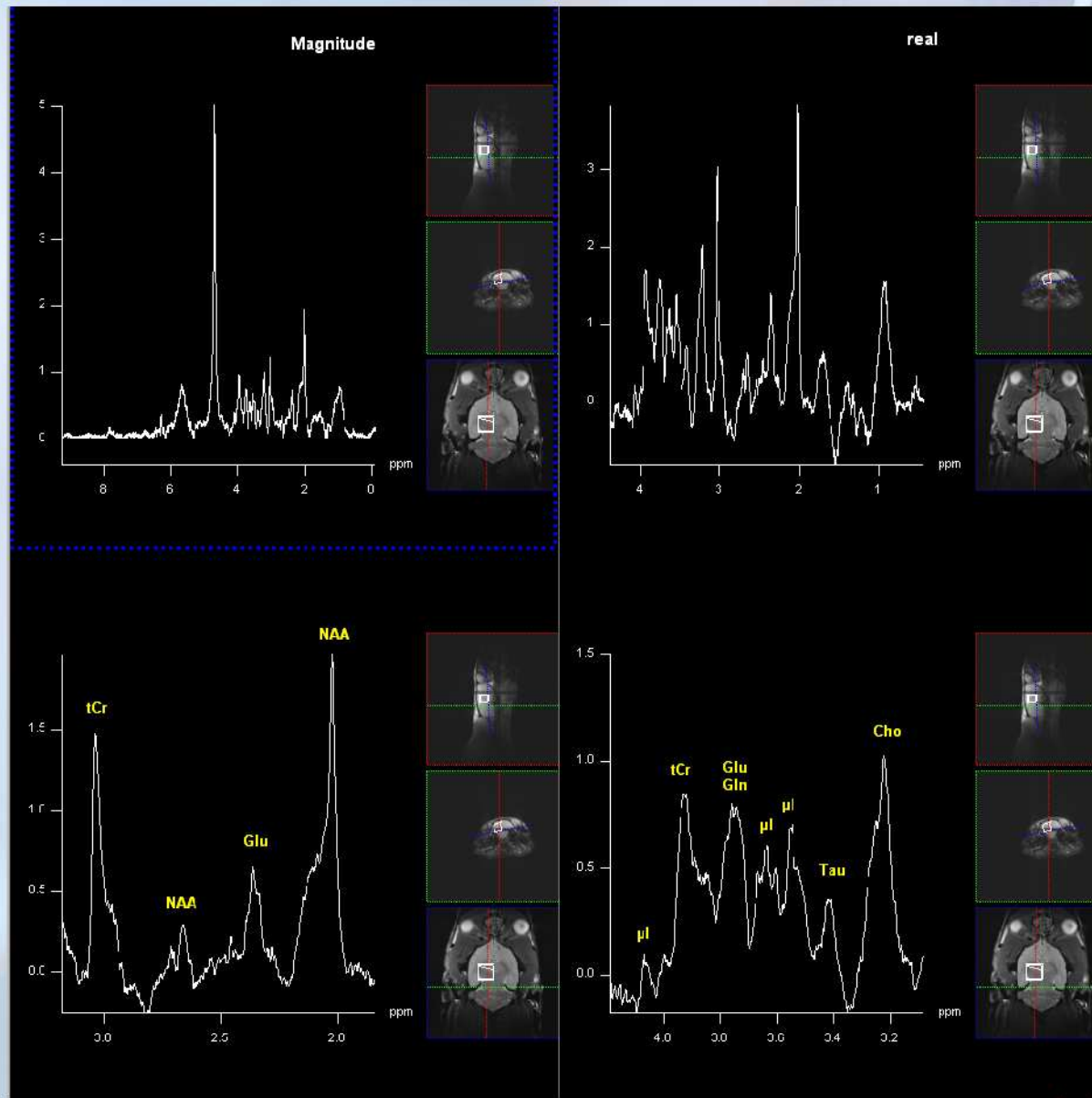


TR: 35 ms  
TE: 1.5 ms  
Flip Angle: 30°



Slice Thickness: 1.5 mm  
Matrix: 256 × 256

# Spectroscopy: Short Echo Time STEAM

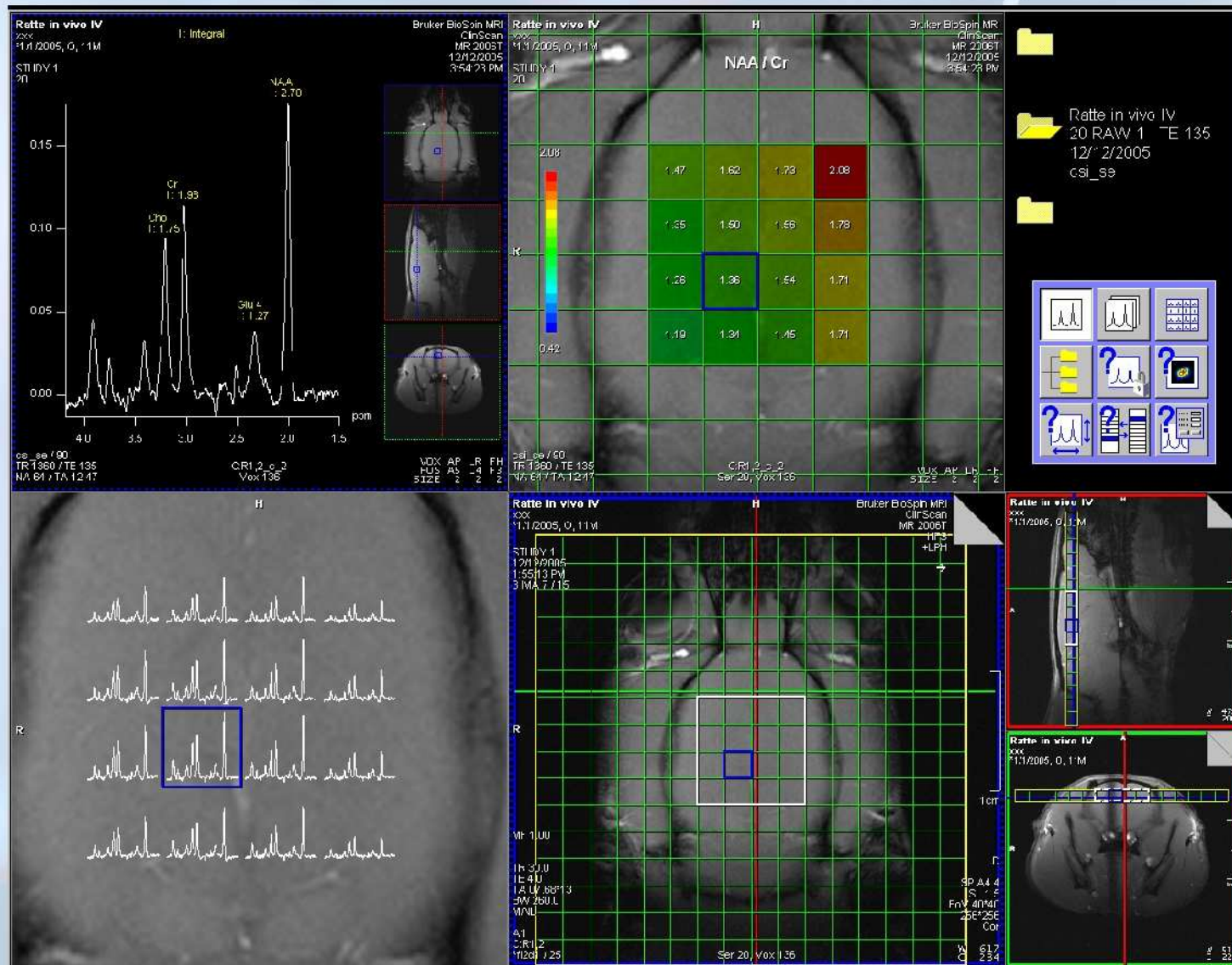


TE 3 ms

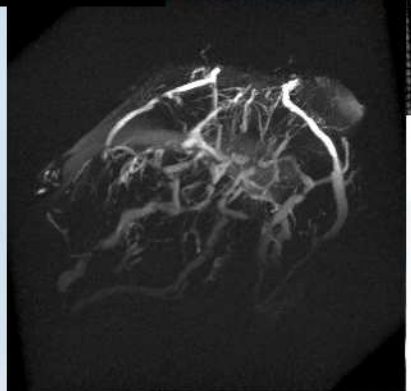
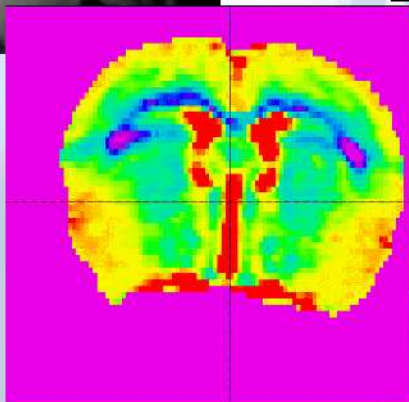
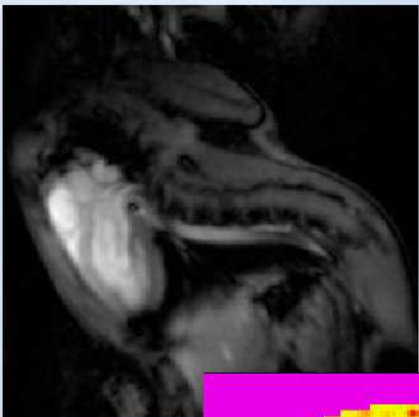
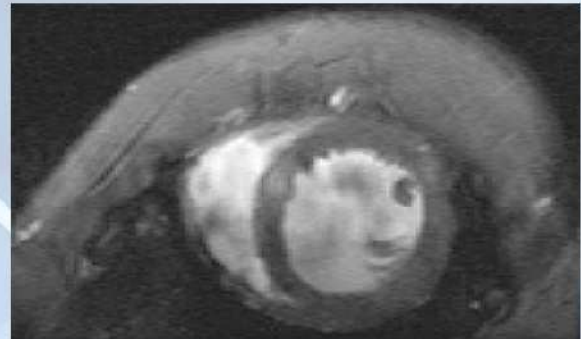
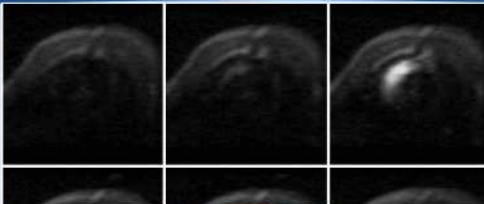
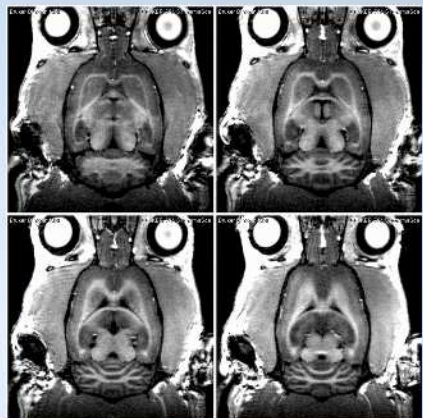
$4 \times 4 \times 4 \text{ mm}^3 = 64 \mu\text{l}$

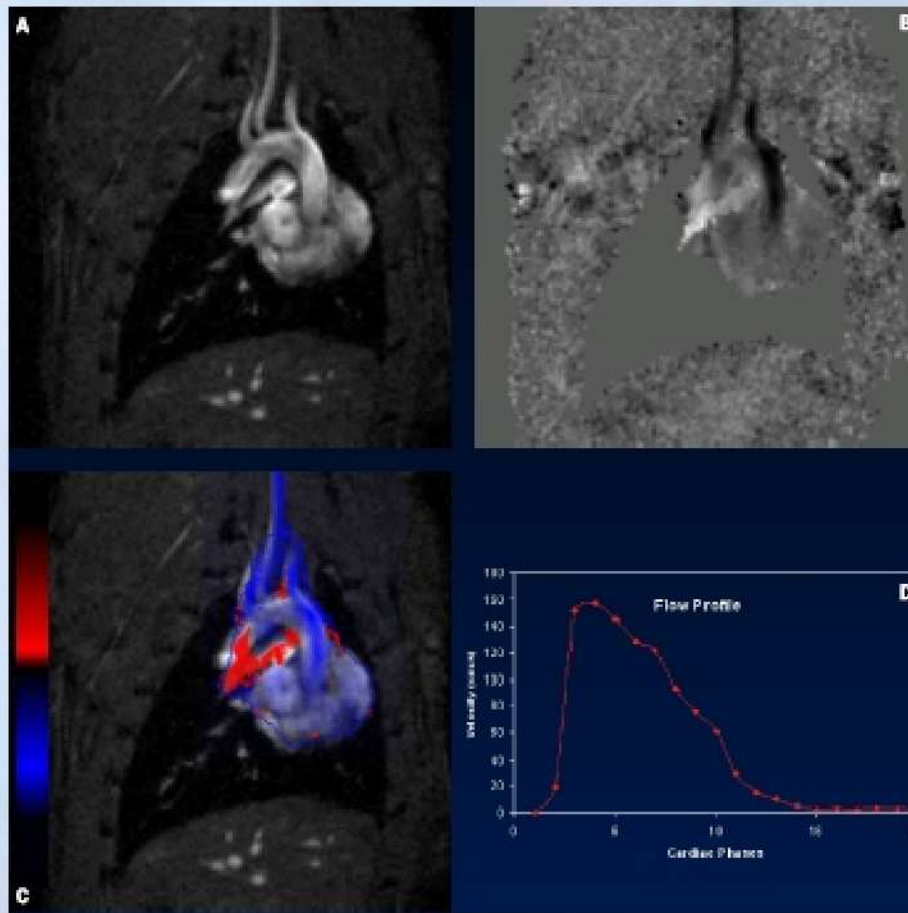
scan time 3:12 min

# Spectroscopy: Hybrid CSI PRESS



# BioSpec® & PharmaScan® Summary





Rat Heart (*in vivo*)  
FLOWMAP

TR: 9 ms  
TE: 2.8 ms  
Slice Thickness: 1.2 mm  
FOV: 4.8 cm  
Matrix: 128×128  
Frames: 20

TET: 3:00 min

Coil:  
60 mm linear T/R

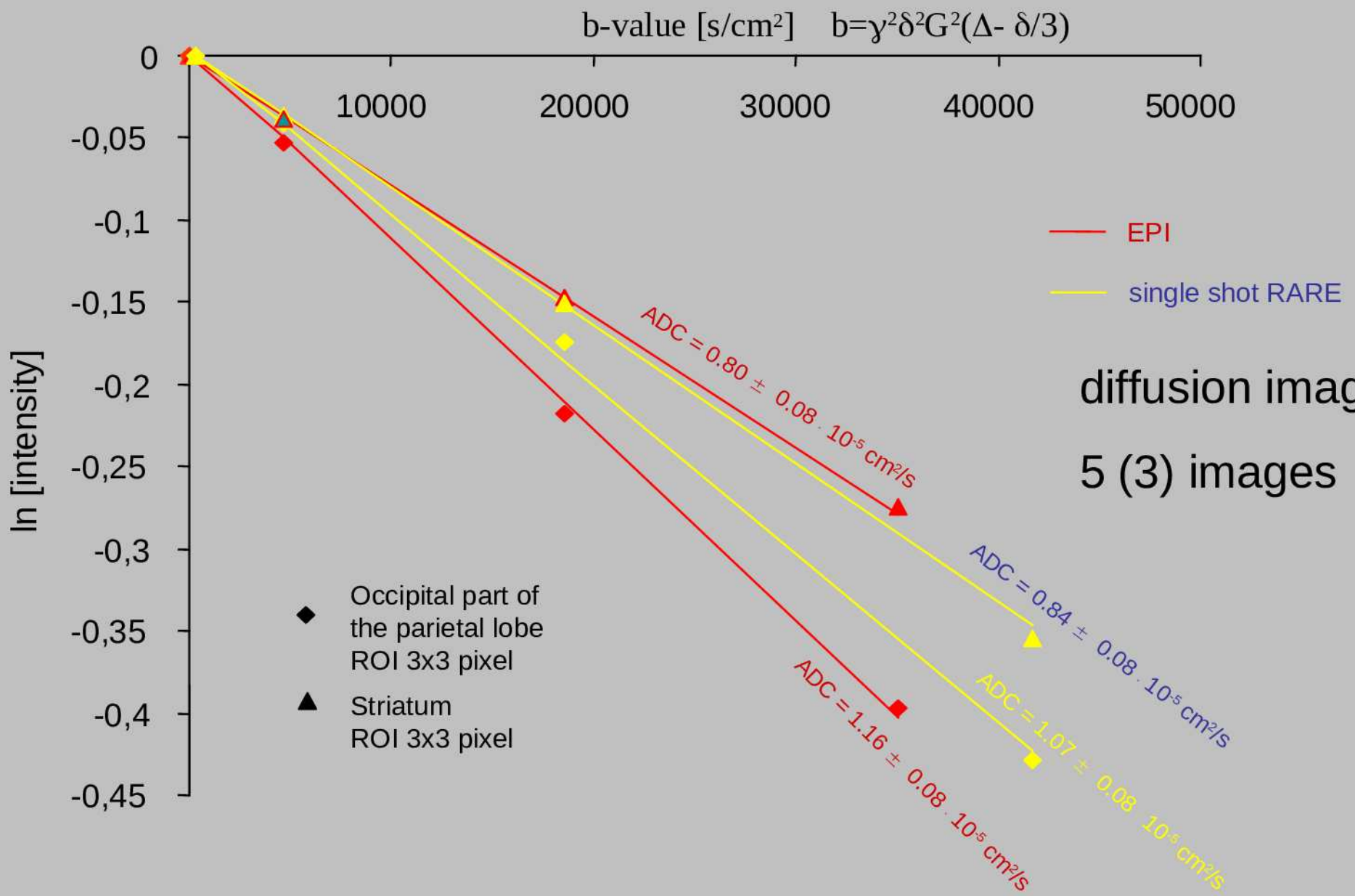
Blood Flow = Flow comp. - Flow deph.

# Diffusion

# Perfusion

# Imaging

# data analysis



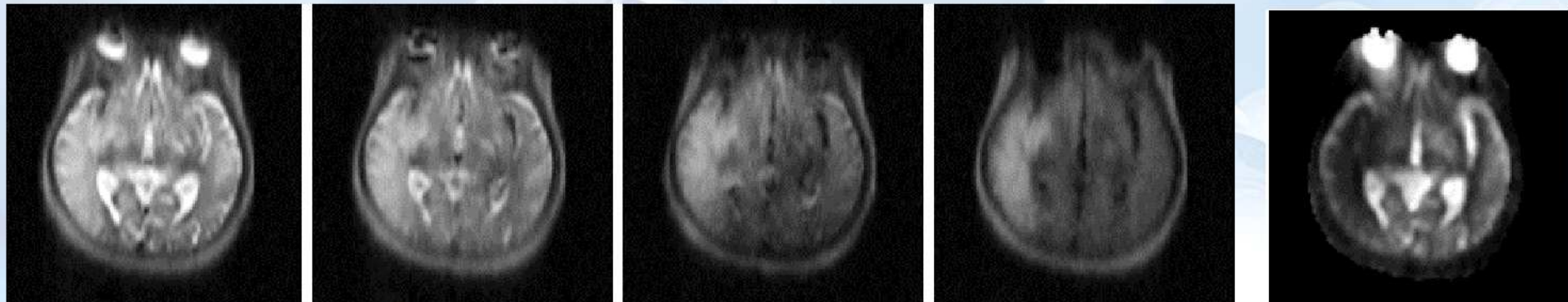
# Clinical Applications



## Acute right MCA Stroke

Diffusion weighted single shot RARE imaging provides anatomically accurate images, i.e. without the usual distortions seen on diffusion weighted EPI, which are caused by susceptibility artifacts close to e.g. sinonasal cavities.

### Diffusion weighted single shot RARE imaging



$b = 480 \text{ s/cm}^2$

$b = 7730 \text{ s/cm}^2$

$b = 30915 \text{ s/cm}^2$

$b = 69550 \text{ s/cm}^2$

ADC map

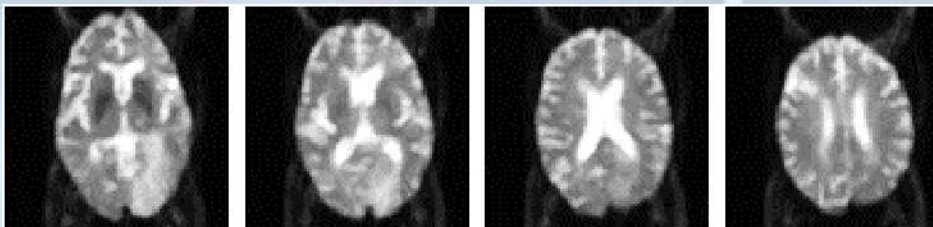
$\Delta = 80\text{ms}$   $\delta = 15\text{ms}$   $G = 2/8/16/24 \text{ mT/m}$

# Stroke: Occipital lobe infarct

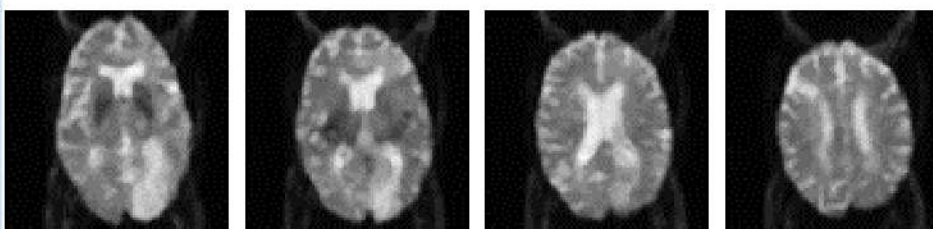


Diffusion weighted spin-echo EPI:  $\Delta = 50$  ms,  $\delta = 15$  ms

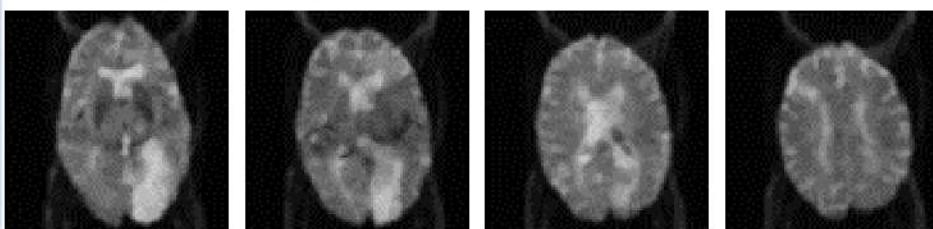
$G = 0$  mT/m



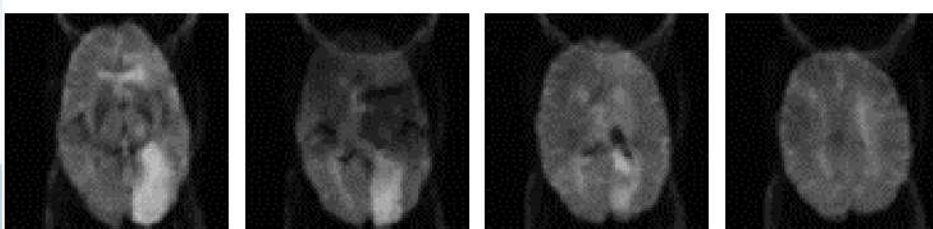
$G = 8$  mT/m



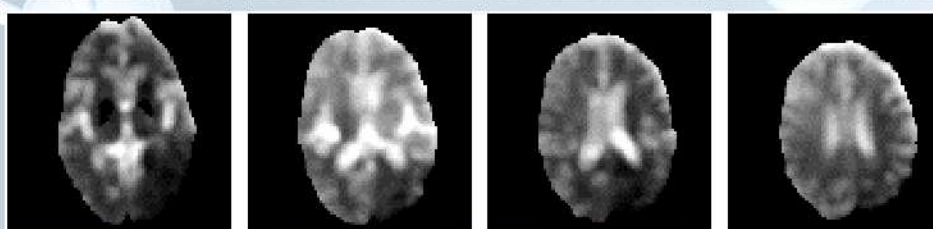
$G = 16$  mT/m

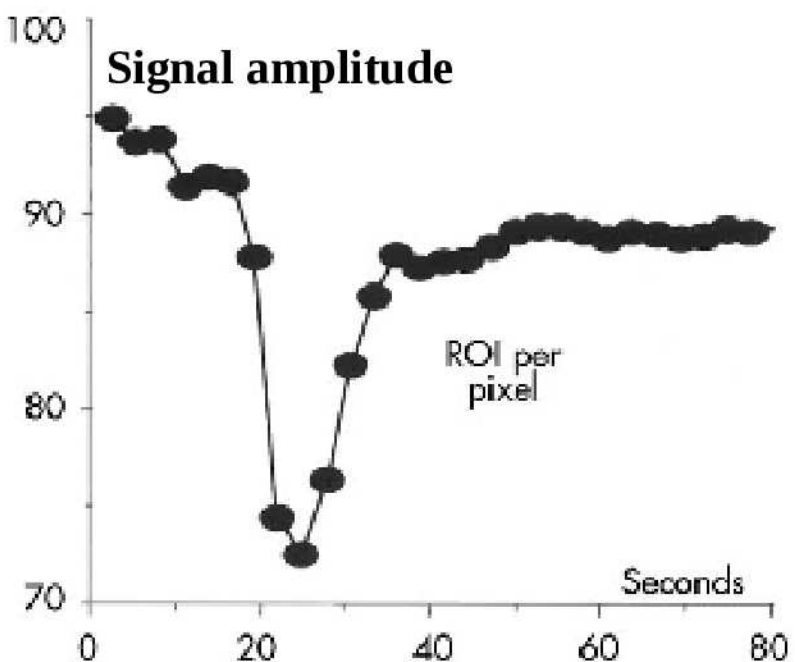
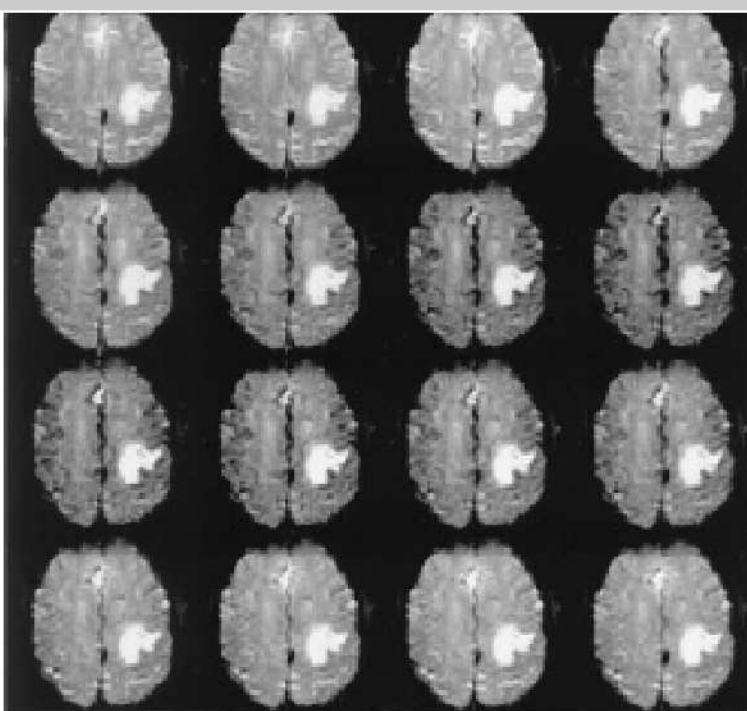


$G = 22$  mT/m

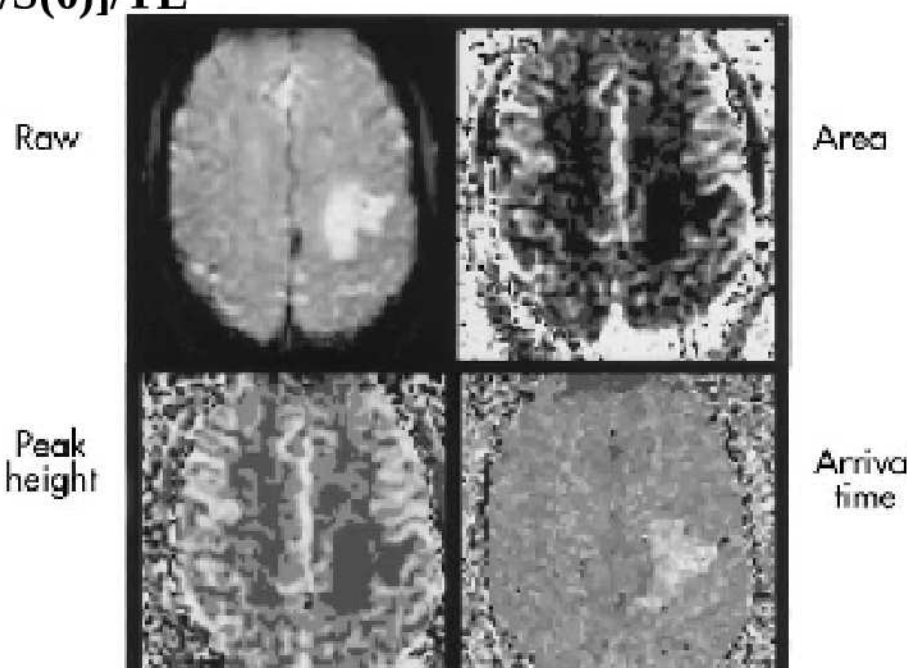
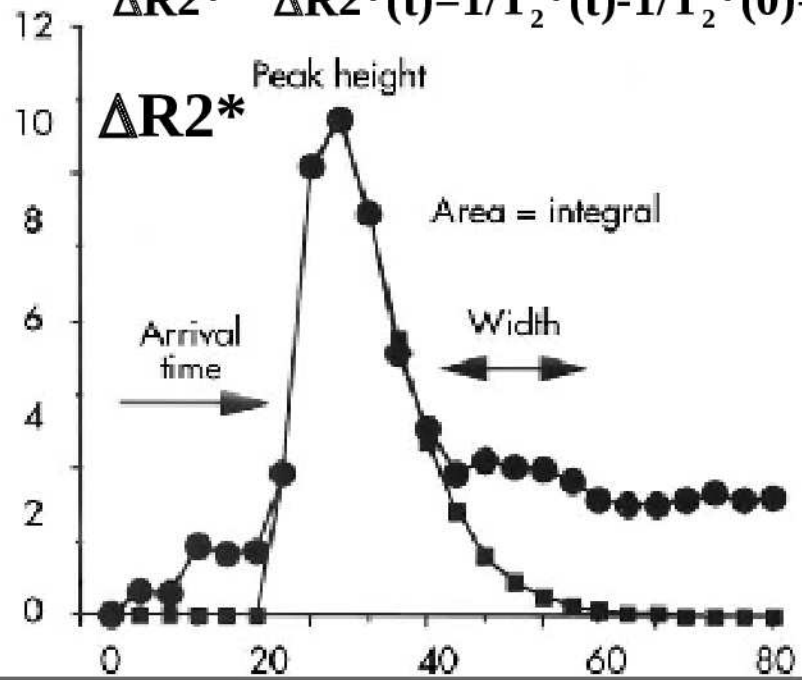


ADC map





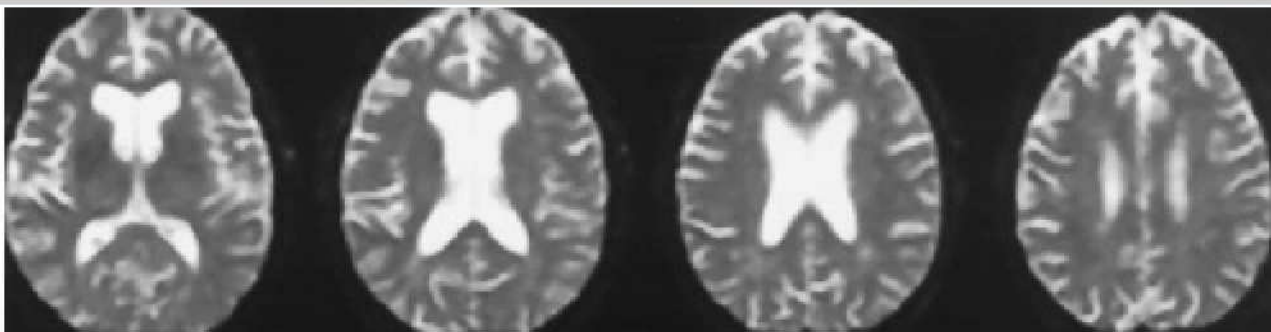
$$\Delta R2^* \quad \Delta R2^*(t) = 1/T_2^*(t) - 1/T_2^*(0) = -\log[S(t)/S(0)]/TE$$



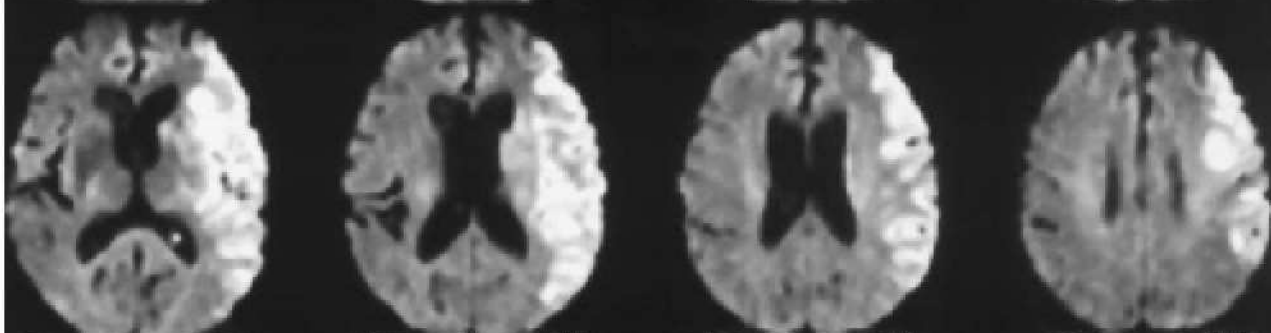
# Comparison of diffusion- and perfusion-weighted images



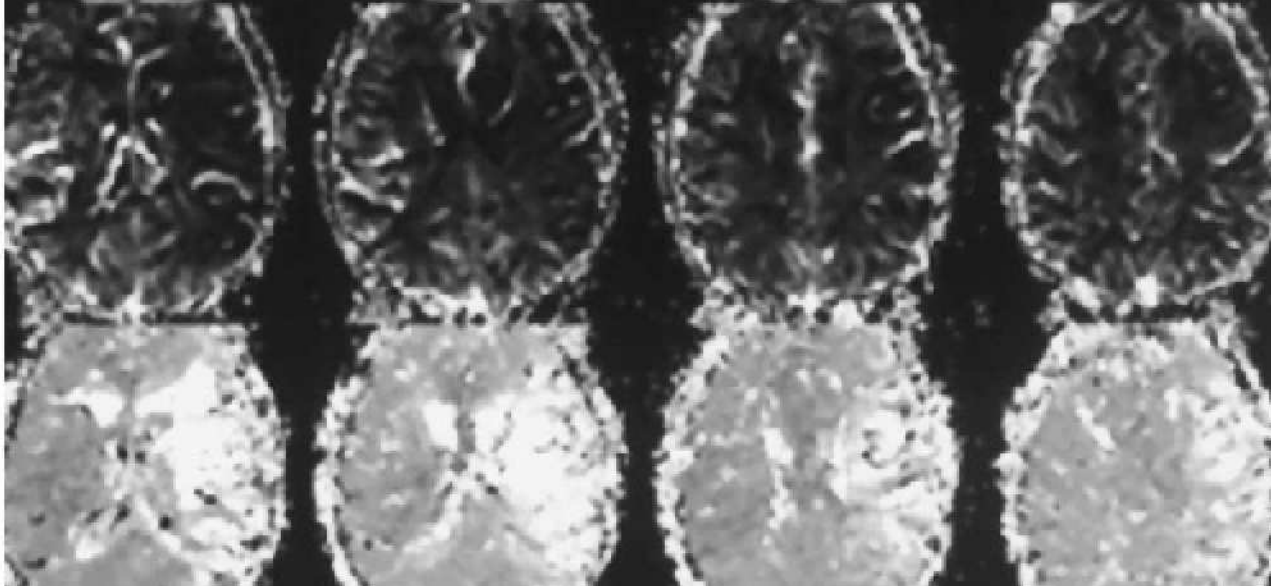
T2



DWI  
881



rCBV



TTP

BRUKER  
BIOSPIN

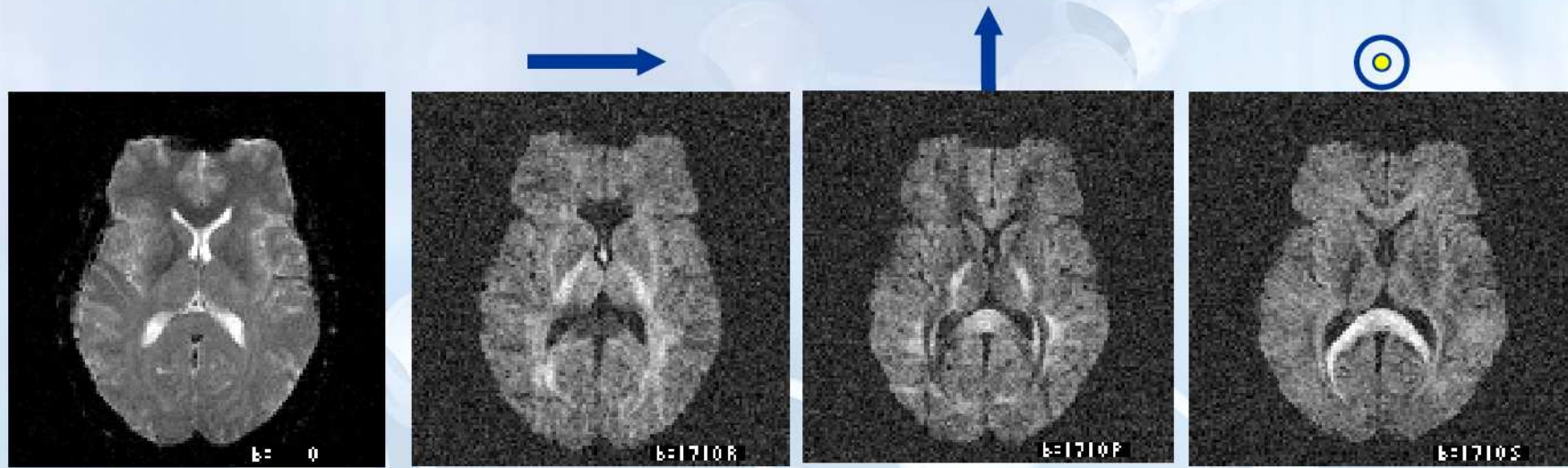
# Diffusion

## Tensor

# Imaging

# Direction dependent contrast

Diffusion weighting in different diffusion encoding directions



DWI images

No DW

DW along  
Read

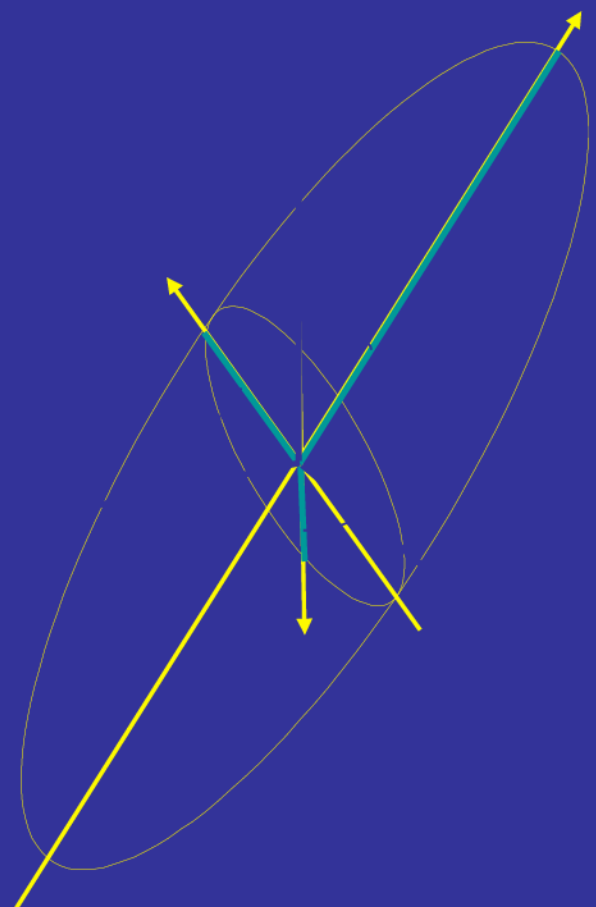
DW along  
Phase

DW in Slice  
direction

-> DWIs show anisotropy and are rotationally variant,  
i.e. SI is dependent on the patients' head position!

# Diffusion Tensor

5(3)x10(5) images



Directional dependence of diffusion can be described with a Tensor with 6 independent components

$$DT = \begin{bmatrix} D_{xx} & D_{xy} & D_{xz} \\ D_{xy} & D_{yy} & D_{yz} \\ D_{xz} & D_{yz} & D_{zz} \end{bmatrix}$$

$$DT = [v_1 \ v_2 \ v_3]^T \begin{bmatrix} \lambda_1 & 0 & 0 \\ 0 & \lambda_2 & 0 \\ 0 & 0 & \lambda_3 \end{bmatrix} [v_1 \ v_2 \ v_3]$$

Eigenvectors  
Orientation of DT

Eigenvalues  
Form of DT

# Mean diffusivity and anisotropy indexes

Fractional anisotropy :

$$FA = \sqrt{[(I_1 - I_{\bar{I}})^2 + (I_2 - I_{\bar{I}})^2 + (I_3 - I_{\bar{I}})^2] / I_{\bar{I}}^2}$$

Mean diffusivity

$$D' = \text{Trace}(DT)$$

Anisotropy indexes:

Fractional anisotropy

$$0 \leq FA \leq 1$$

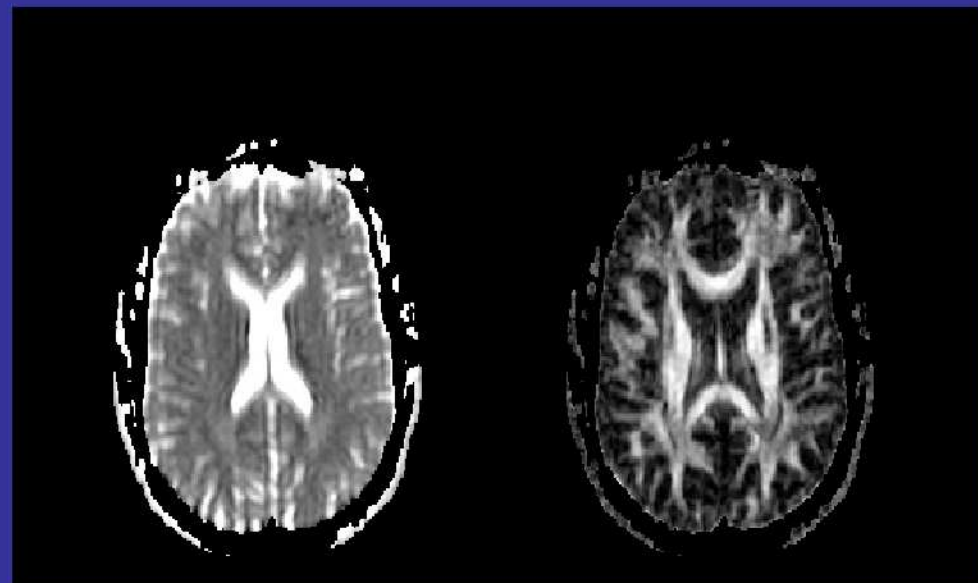
- apparent anisotropy  
 $(ADC_x - ADC_y) / ADC_x$

- Relative anisotropy

$$0 \leq RA \leq 2^{1/2}$$

- Volume ratio  $1 \geq VR \geq 0$

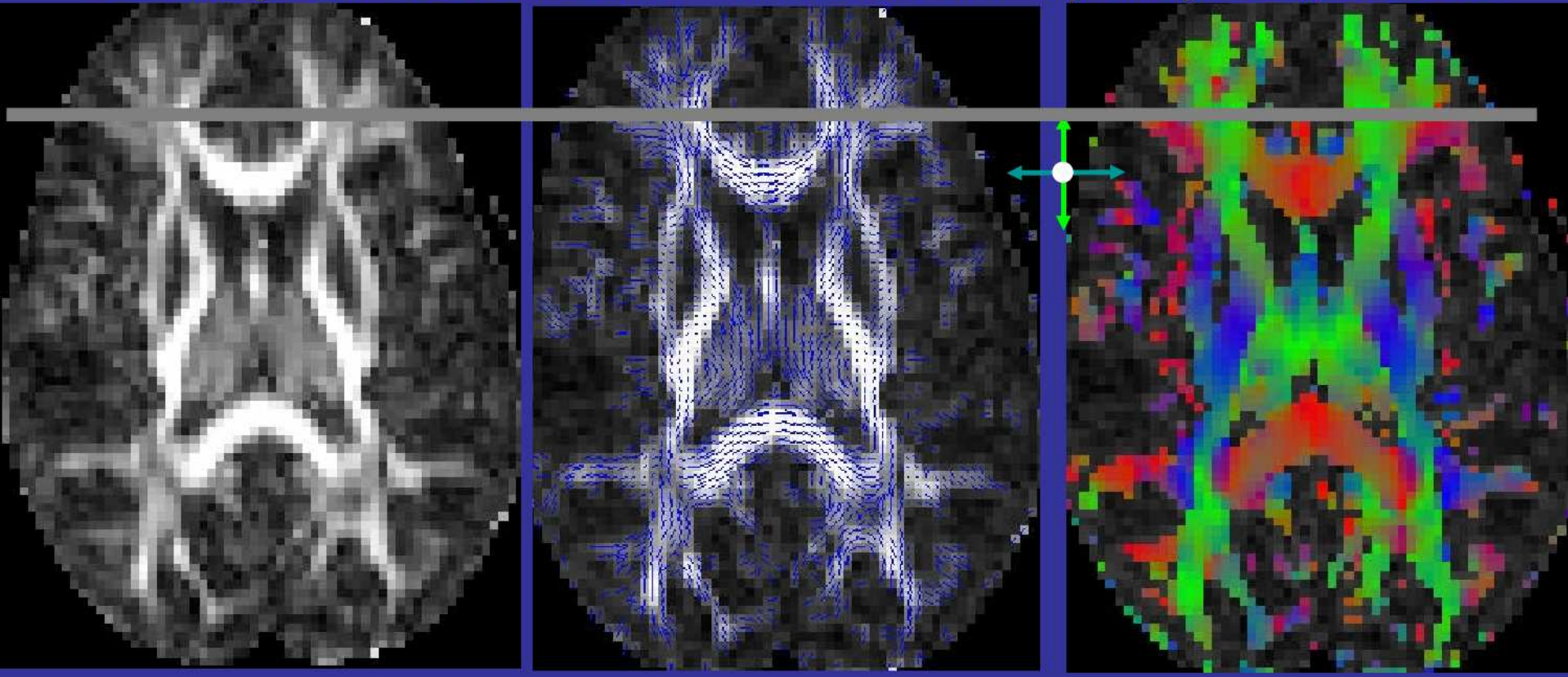
- Diffusion Anisotropy  $A\sigma$



K. A. Il'yasov UNIVERSITY  
FREIBURG HOSPITAL

# Fiber orientation mapping

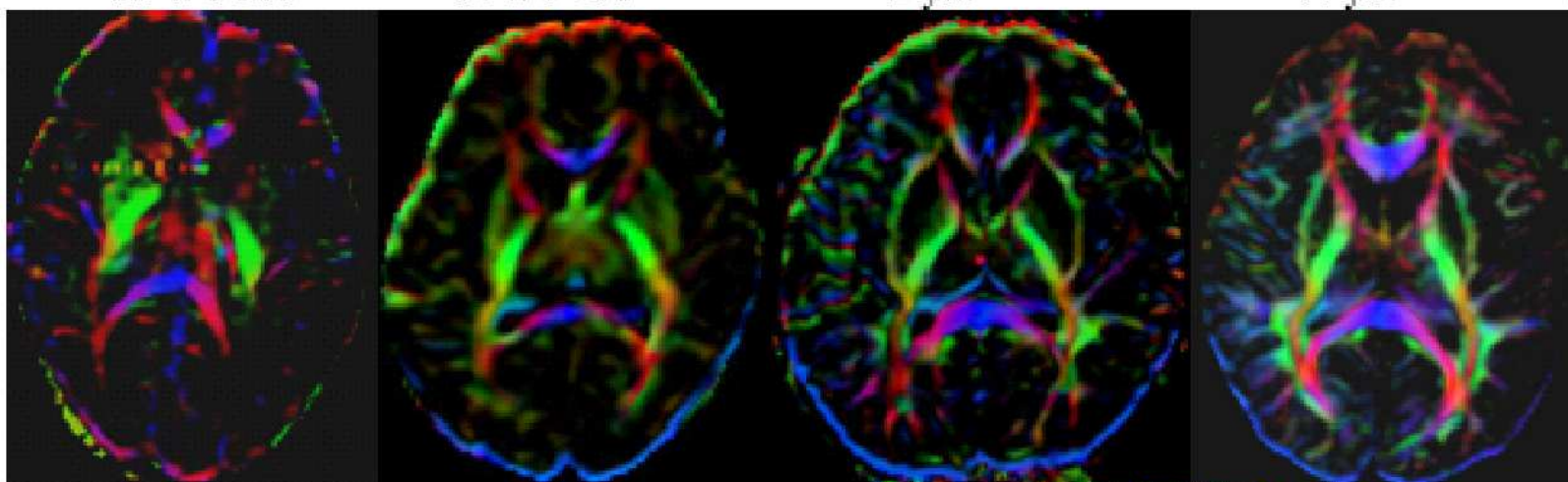
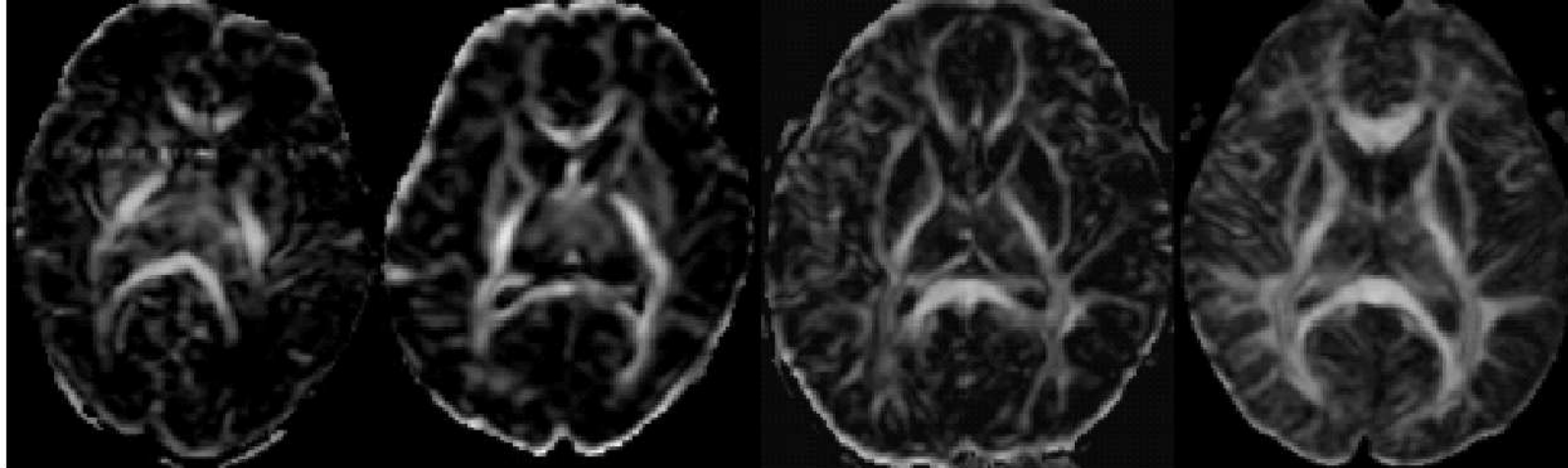
Assumption: fiber direction = direction of the principal eigenvector



FA map

inplane vector map

color-coded map

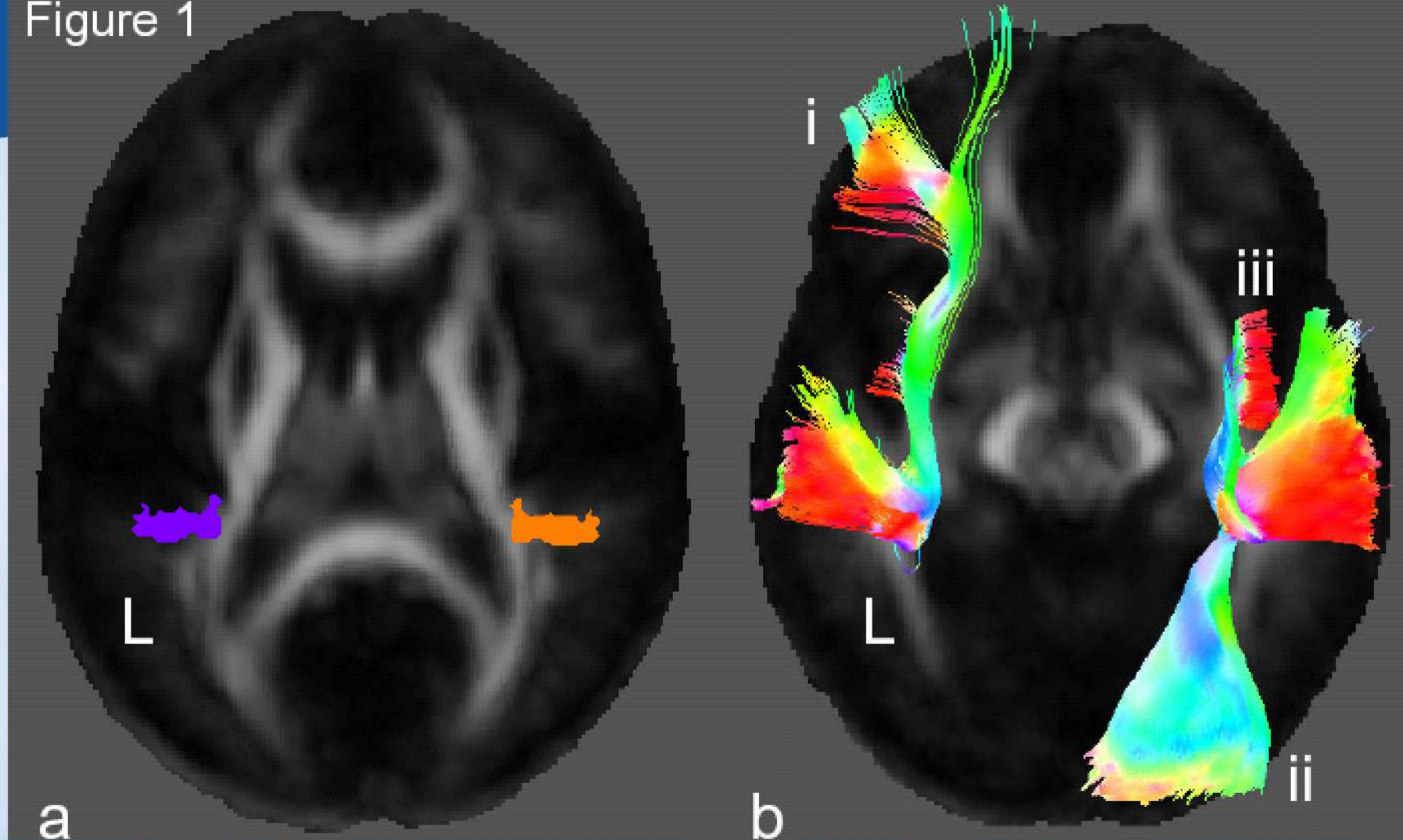


fractional anisotropy in the brain at different age



DDT  
diffusion tensor  
tractography

Figure 1



**white matter pathway assymetry corresponds to auditory spatial and language lateralisation**

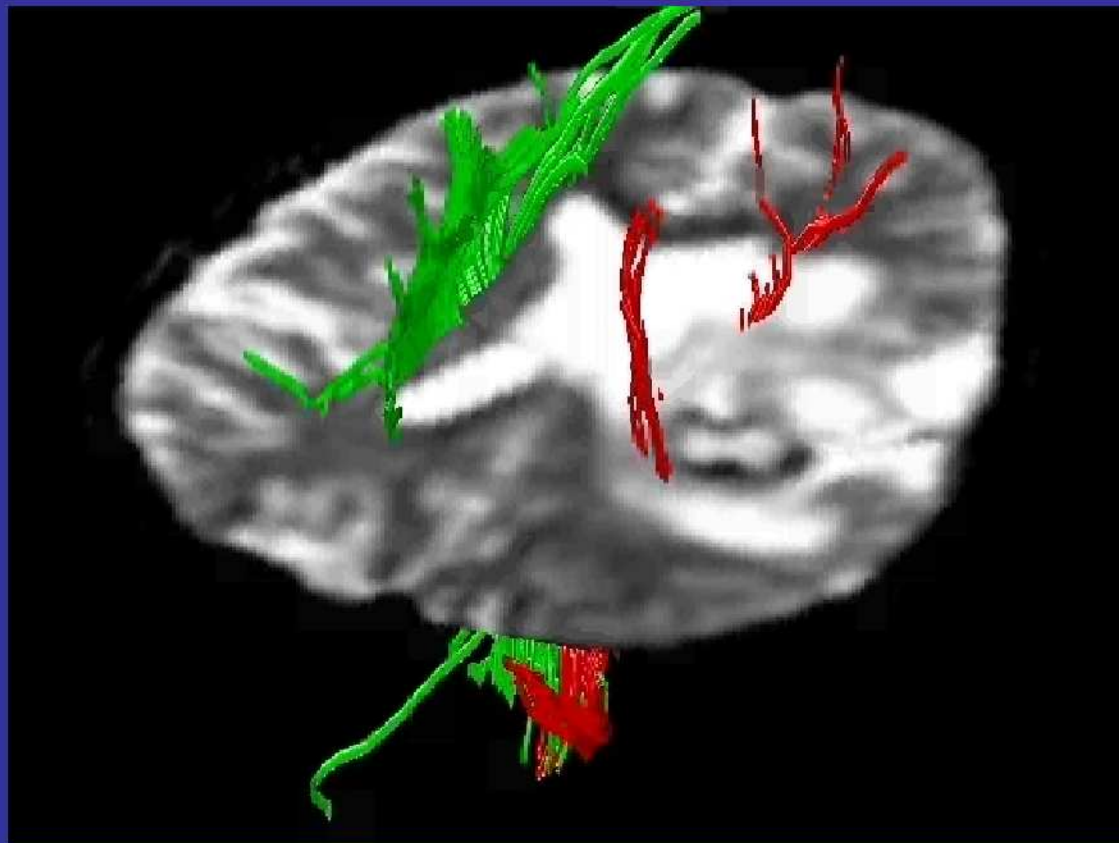
$$\text{fractional asymmetry: } FA = \sqrt{[(\lambda_1 - |\lambda_1|)^2 + (\lambda_2 - |\lambda_1|)^2 + (\lambda_3 - |\lambda_1|)^2]} / |\lambda_1|^2$$

asymmetry in right and lower in left hemisphere

area ii. Parietal and occipital lobe iii. insular cortex

a. greater

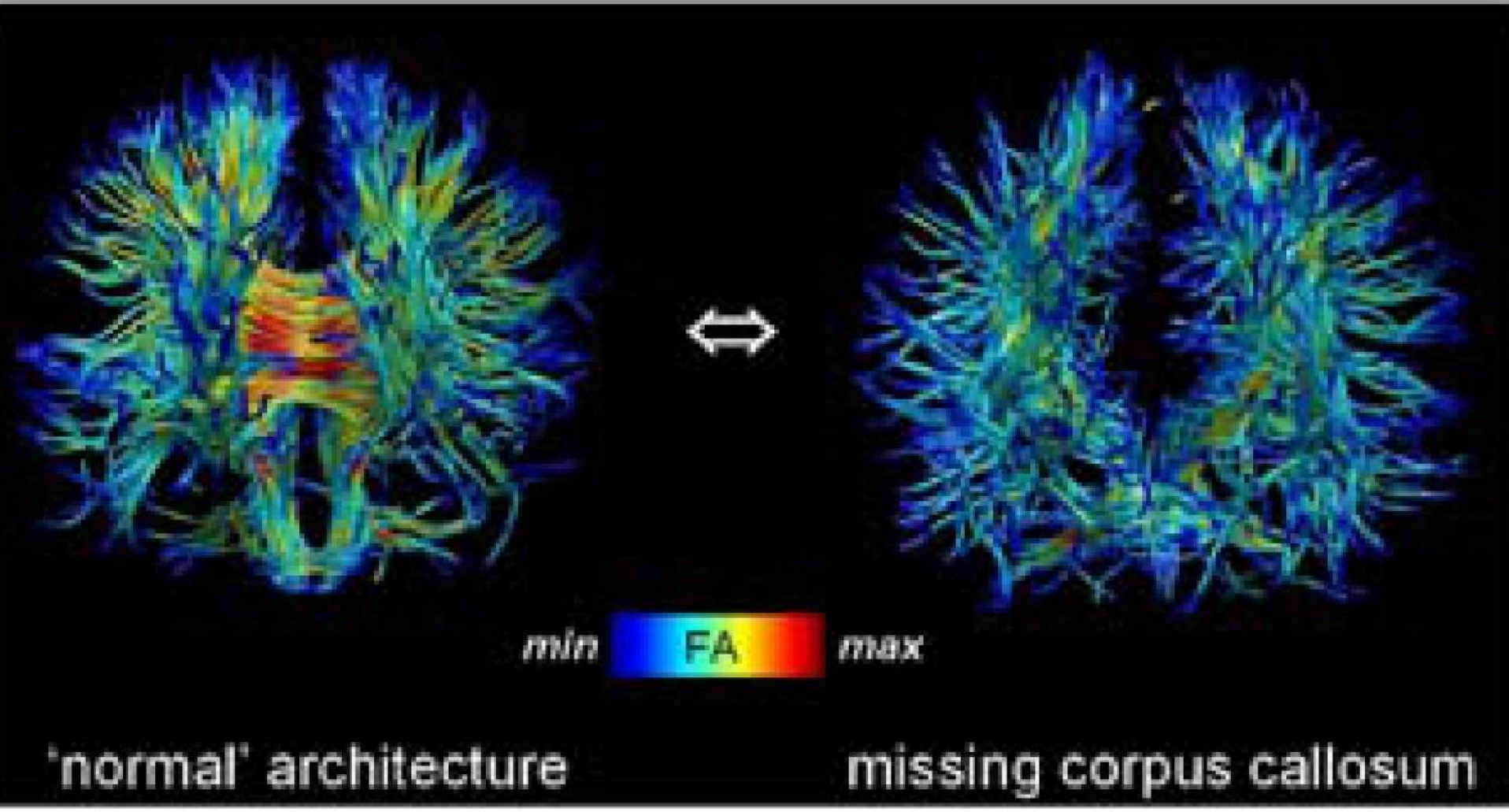
# Patient with brain abscess



Green – healthy  
left side

Red – right side

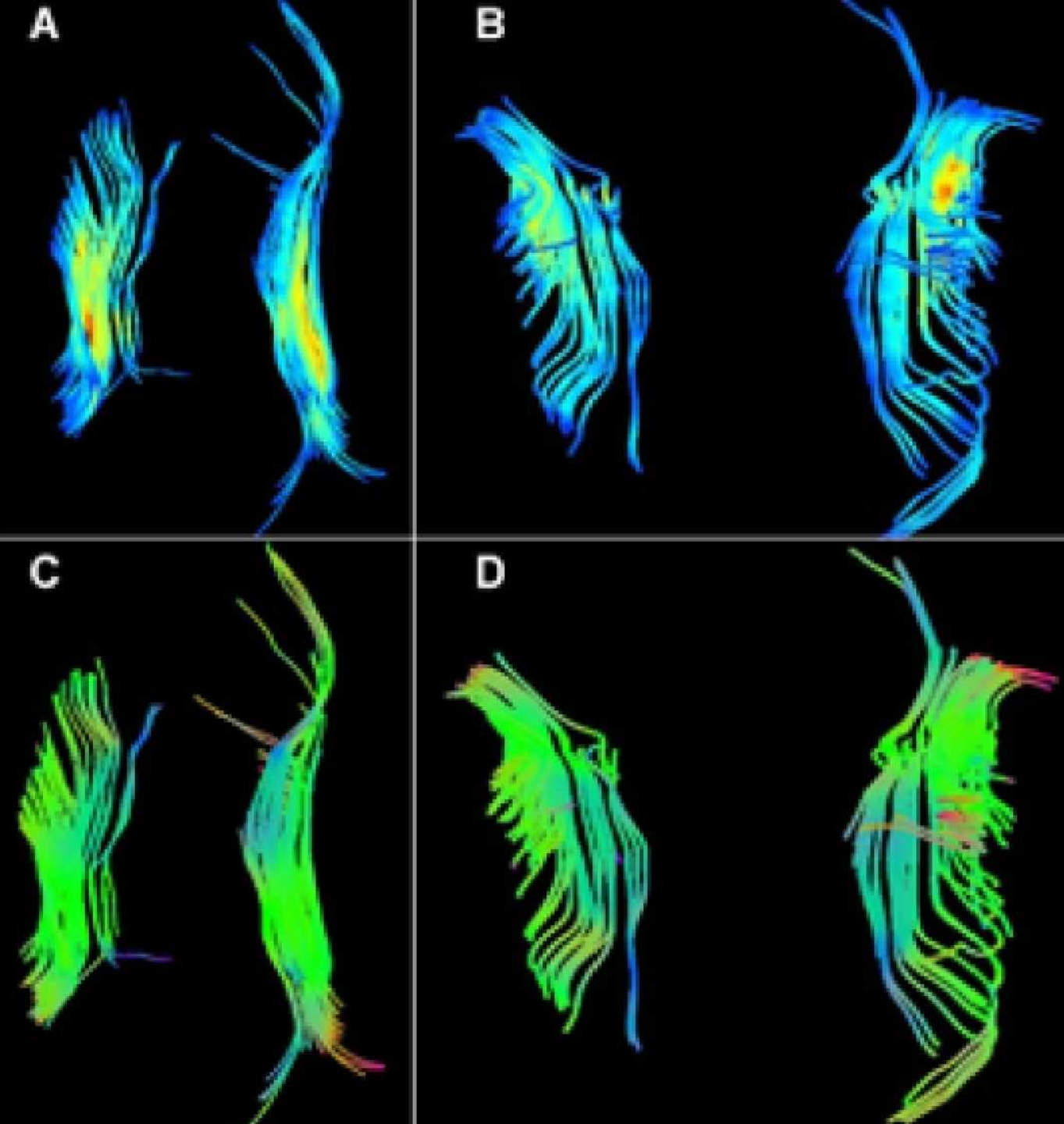
DTI indicates  
damage of motor  
tract, however  
patient does not  
show corresponding  
clinical signs



ESMRMB 2006,49 W. Van Hecke

Diffusion tensor fiber tracking in patients with agenesis of the corpus callosum





ESMRMB 2006,49  
W. Van Hecke

Diffusion tensor fiber  
tracking in patients  
with agenesis of the  
corpus callosum



3D rendering of geometry and fiber structure of a reconstructed heart  
colour coding of

orientation in eigenvector directions of diffusion tensor

blue: fibers in circumferential  
direction

red: fibers perpendicular to  
circumferential direction along the long axis

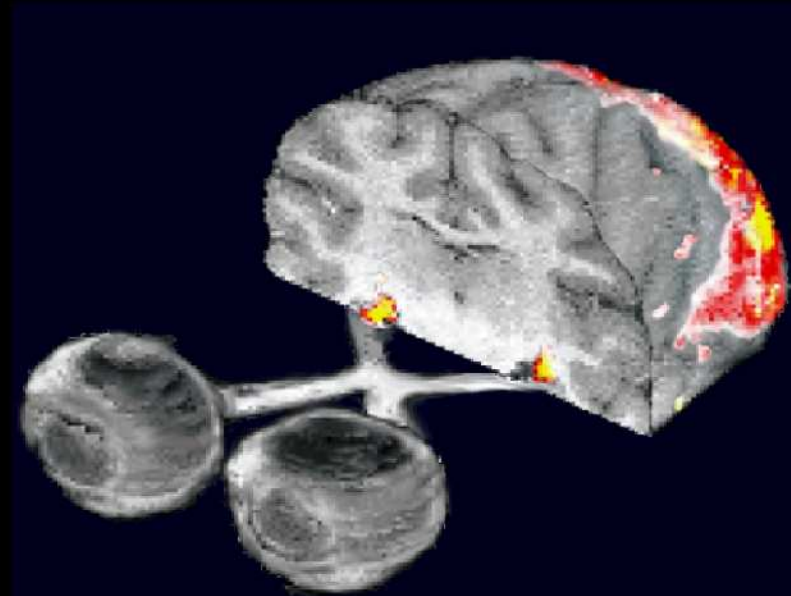
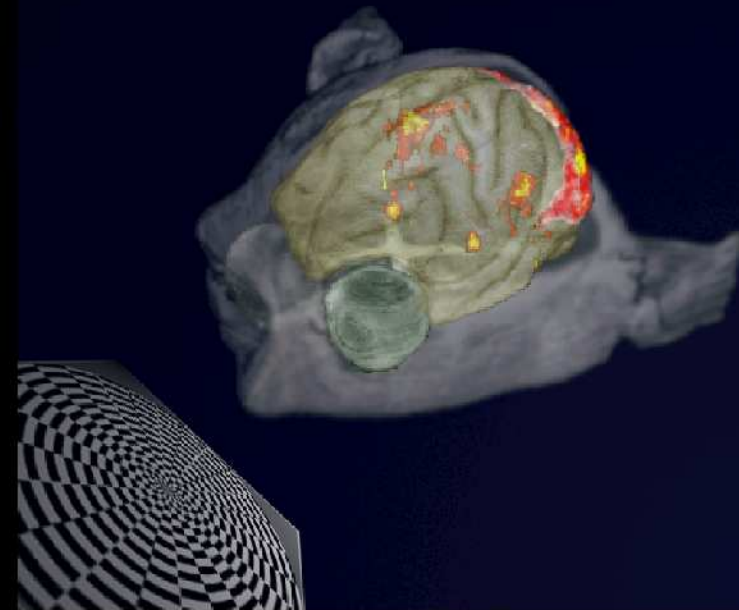
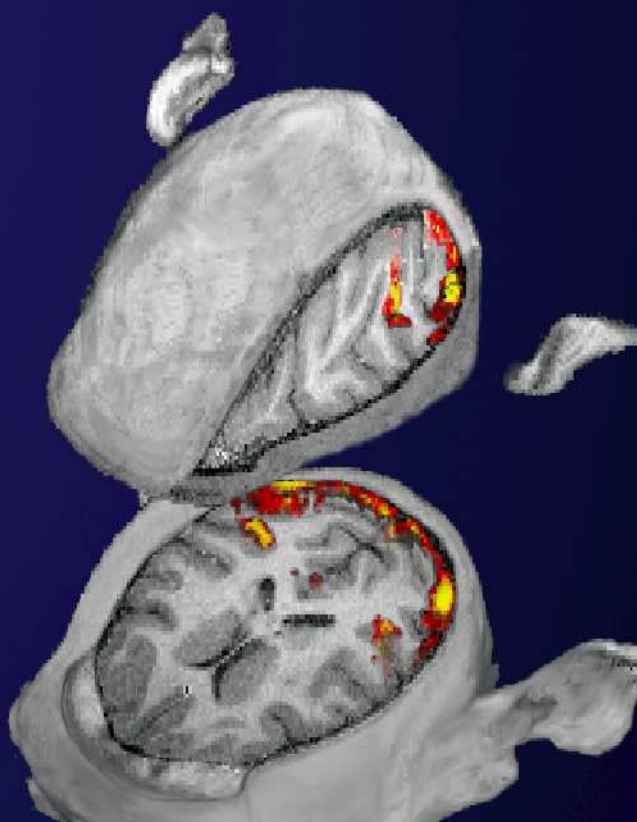
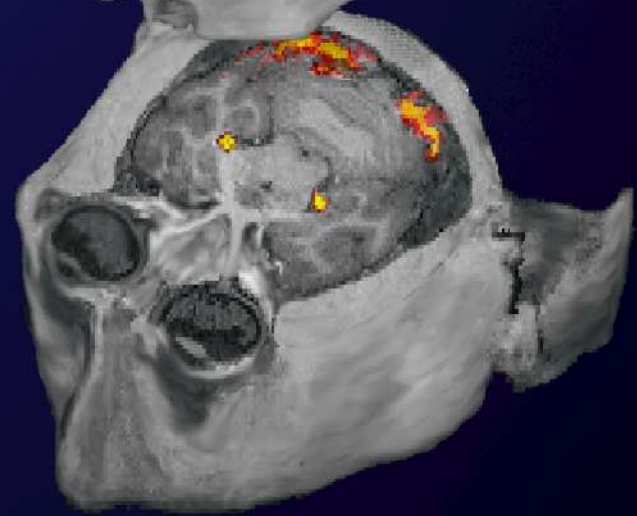
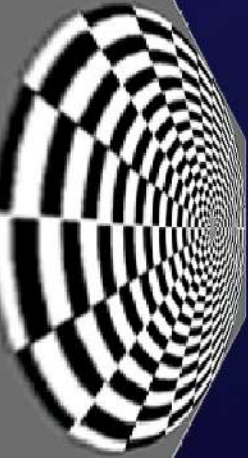
MRM 54(2005)850 P.A.Helm,H.-Tseng,L.Younes,E.R.McVeigh, R.L.Winslow

# functional Imaging

Oxygen consumption  $\Rightarrow$  deoxyhemoglobin  $\uparrow$   
signal decrease ( $T2^*$ )

supply of fresh blood  $\Rightarrow$  oxyhemoglobin  $\uparrow \uparrow$   
signal increase ( $T2^*$ )

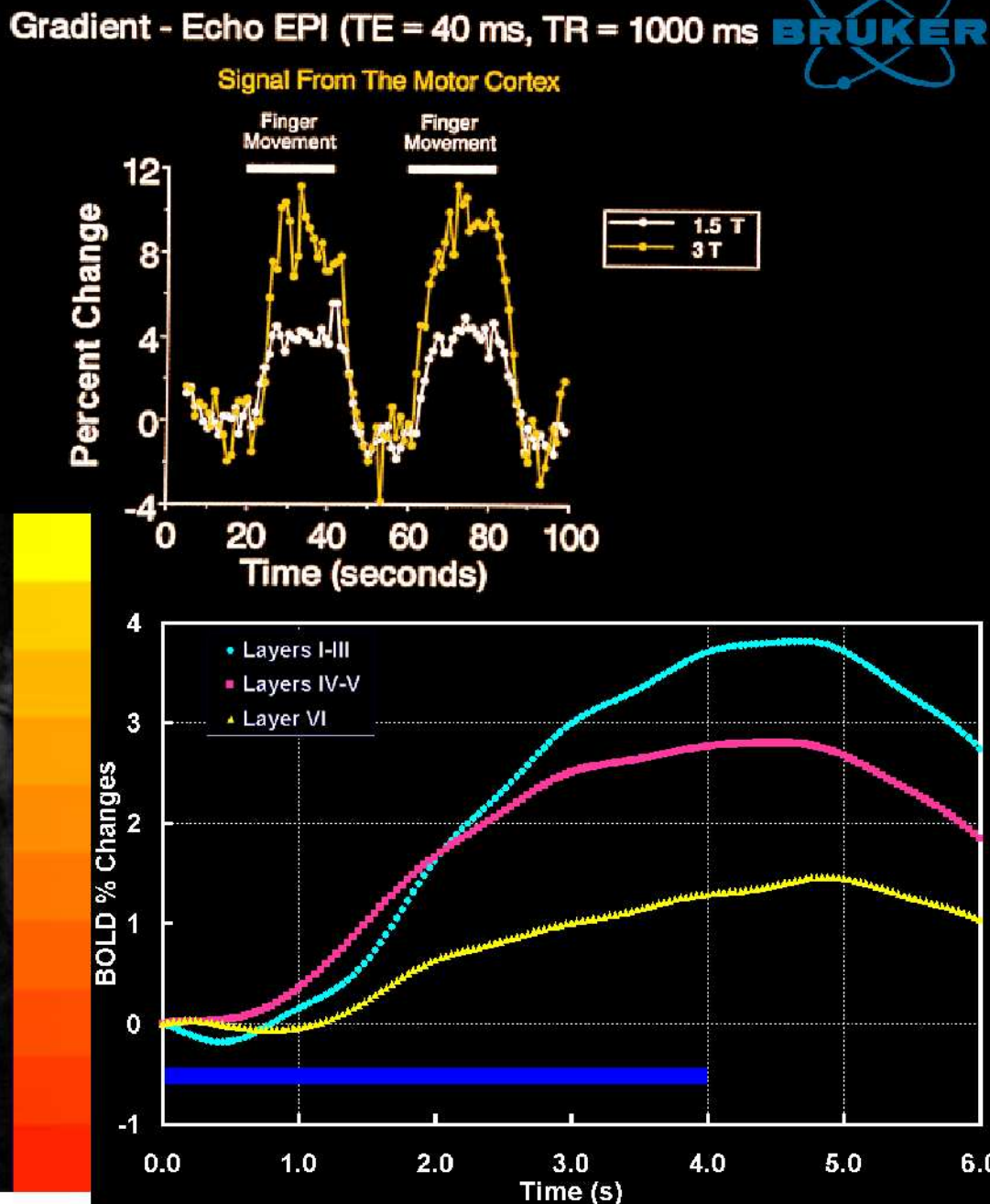
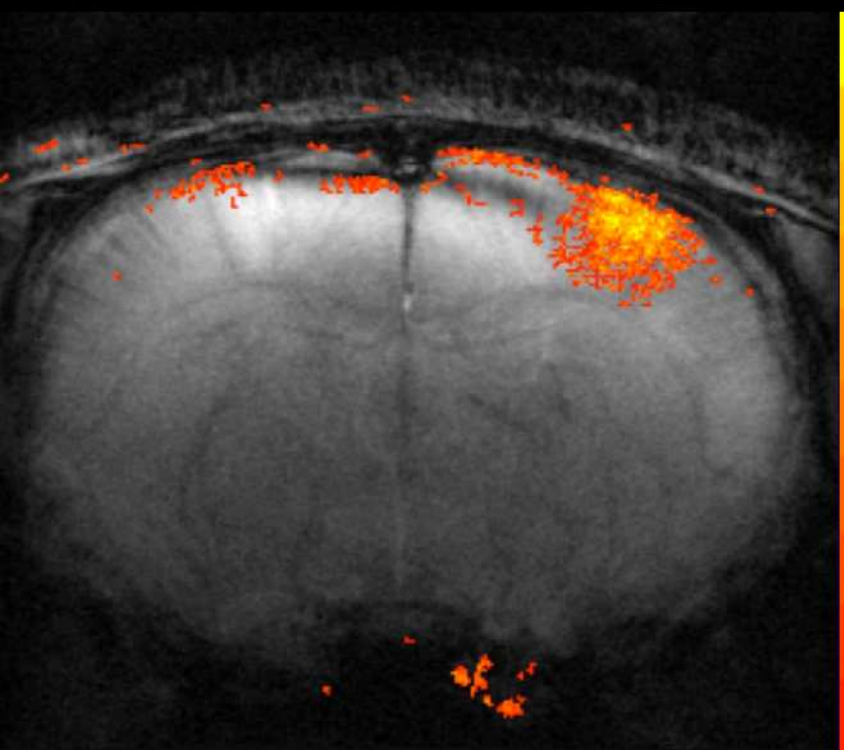
total effect  $\Rightarrow$  oxyhemoglobin  $\uparrow$   
some signal increase (10-30%)



# FIELD STRENGTH COMPARISON: ADVANTAGE OF 3 TESLA

The effect of 3T on the signal changes in fMRI involving the motor cortex, as compared to 1.5T, using gradient-echo echo-planar imaging.

Courtesy of J. Hyde et al,  
Medical College of Wisconsin,  
Milwaukee, USA



  **BOLD fMRI** and time course in individual cortical layers

# fMRI OF EPILEPSY IN RATS

*BioSpec®: fMRI*

BIOSPEC 47/40

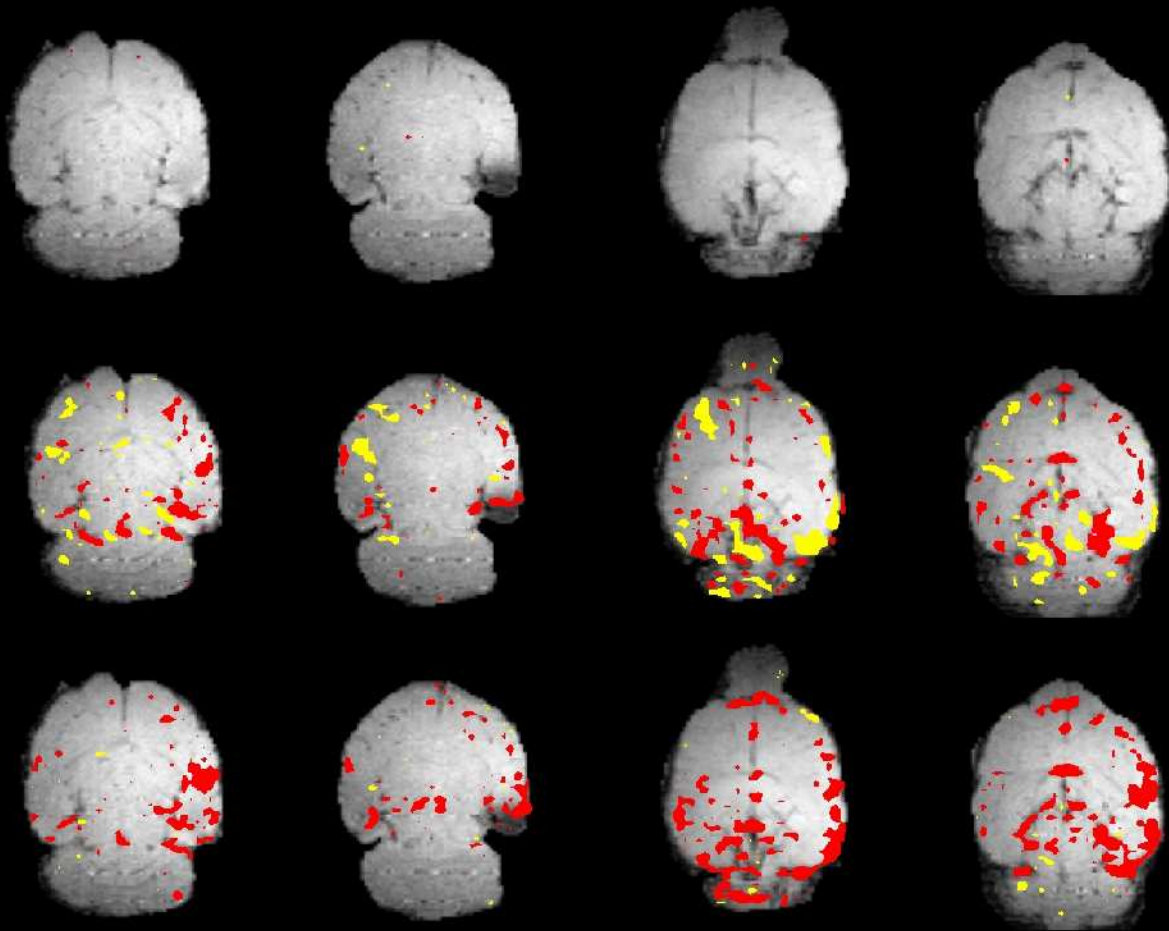
Courtesy and Copyright:

C. Ferris, K. Lahti, D. Olson, J. King

Psychiat. Dept., Univ. Massachusetts, Worcester, USA

Pentylenetetrazol (PTZ) induced epileptic seizures were imaged with BOLD-sensitive GE-MRI ( $TE=20ms$ ). Multiple cortical areas, hippocampal, thalamic and midbrain nuclei show different temporal changes in signal intensity.

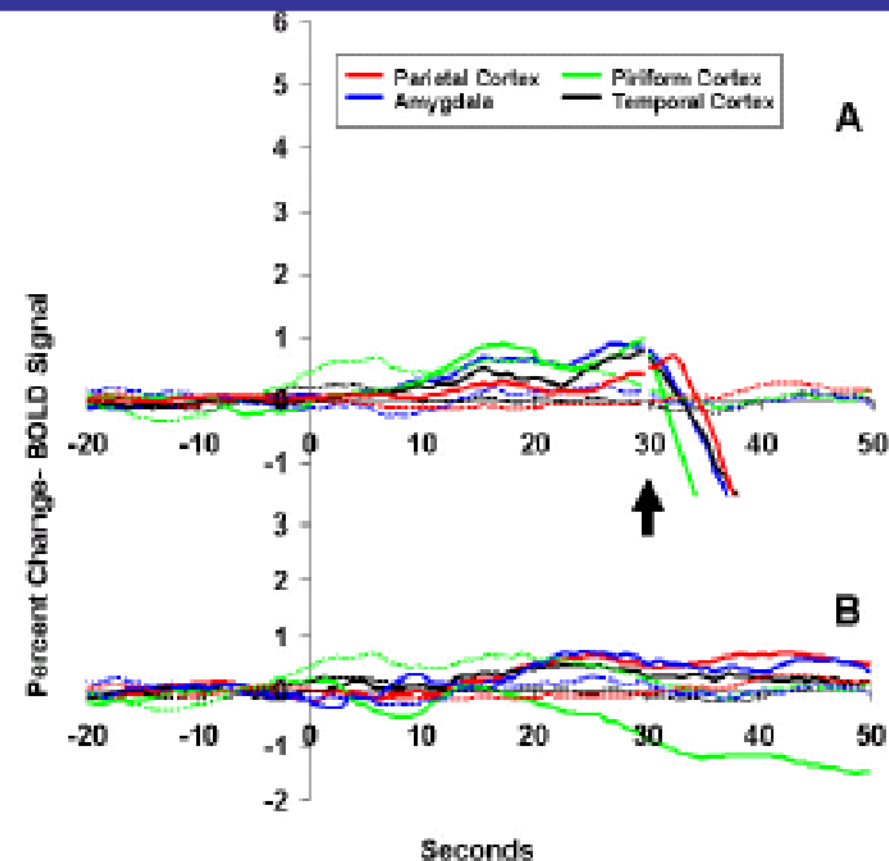
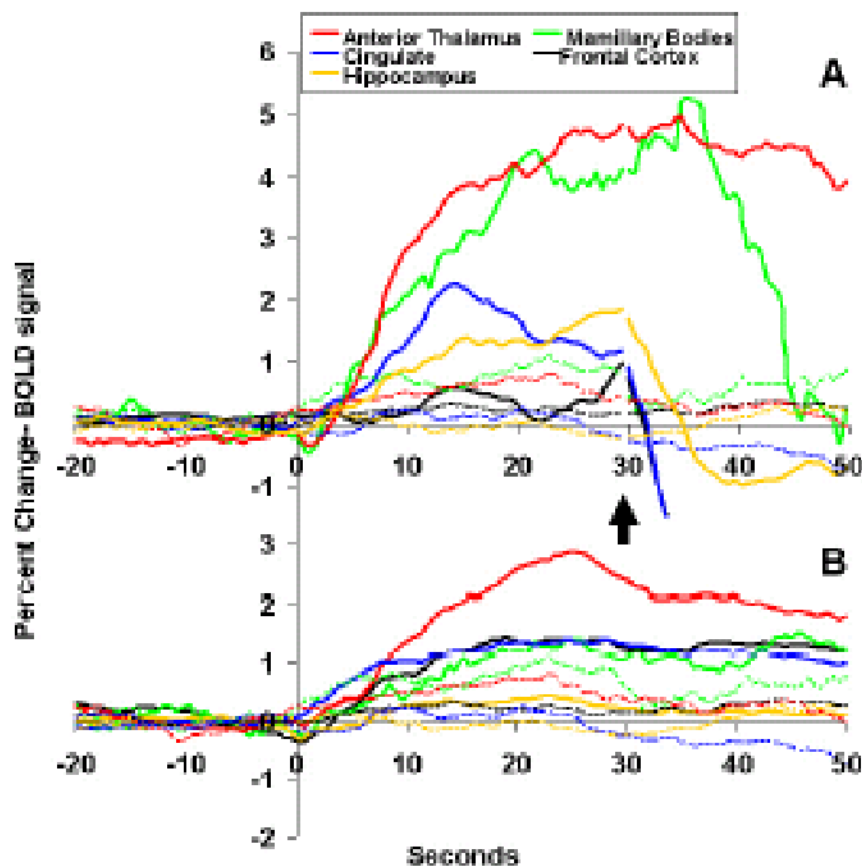
Top row: four slices of the resting state prior to injection; middle row: putative kindling preceding seizure; bottom row: full blown seizure.



Pentylenetetrazol (PTZ) induced epileptic seizures were imaged with BOLD-sensitive GE-MRI ( $TE=20ms$ ). Multiple cortical areas, hippocampal, thalamic and midbrain nuclei show different temporal changes in signal intensity.

Top row: four slices of the resting state prior to injection; middle row: putative kindling preceding seizure; bottom row: full blown seizure.

# Using fMRI to elucidate the Pathways Responsible for Seizure Genesis in a Conscious Animal Model



Epileptic seizures were induced in rats by injection of PTZ. Some rats were treated with a relaxing agent Ethosuximide (ESM).

A: before B: after ESM treatment

arrow indicates onset of seizure

# fMRI reveals declined activation of prefrontal cortex in epilepsy patients on topiramate therapy

BROKER

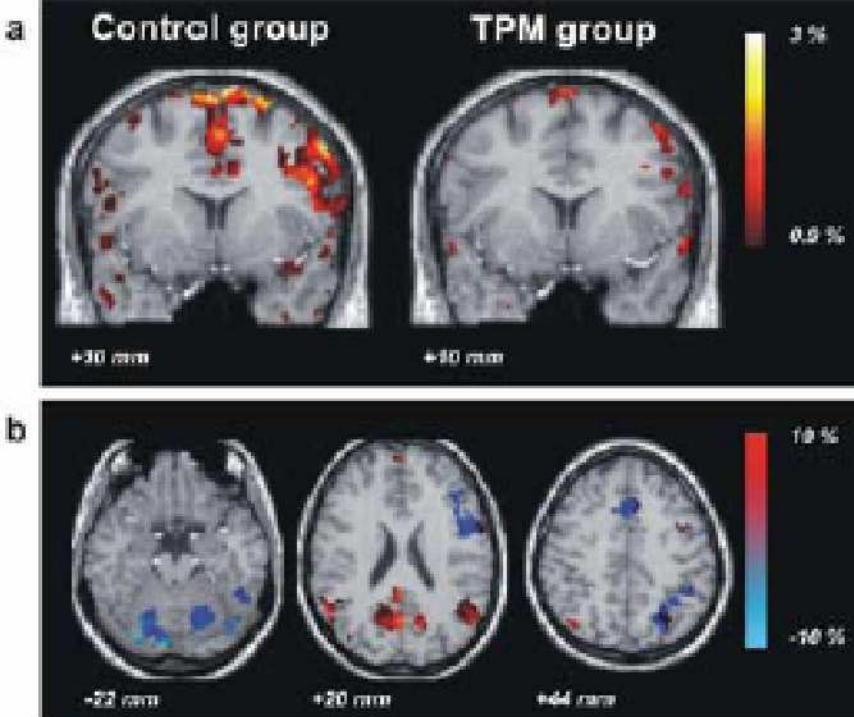


Fig.3: a) Coronal images of group mean functional MRI activation maps, obtained for the covert word generation paradigm overlaid on a normalized T1-weighted MR image, with left the control group, and right the topiramate group. b) Transverse images of average underactivation level for the whole brain of the TPM group as compared to the control group.

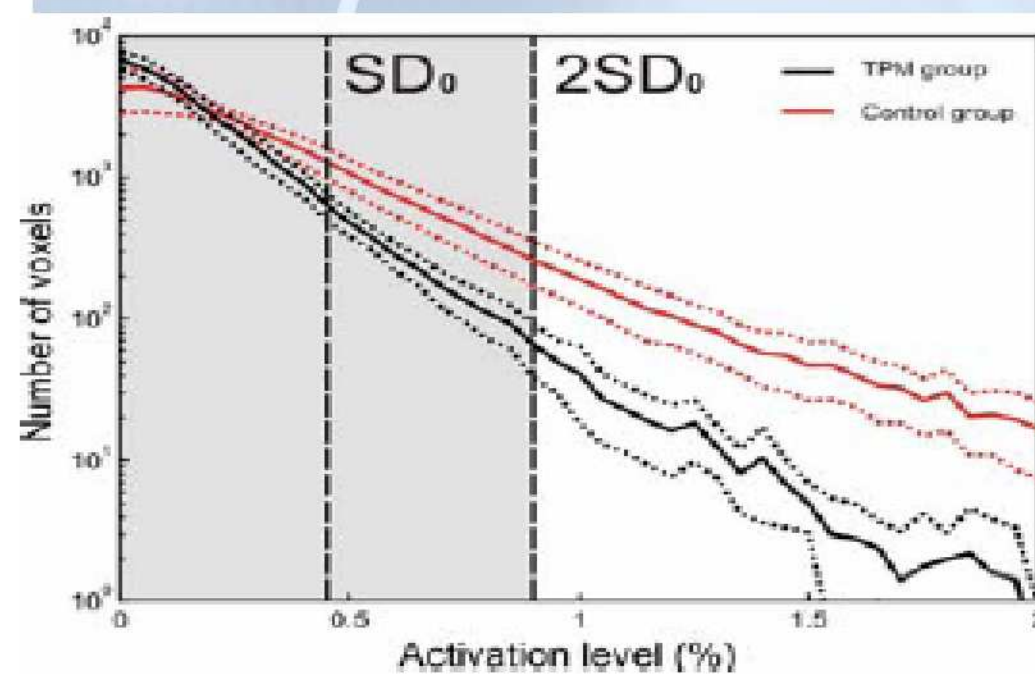
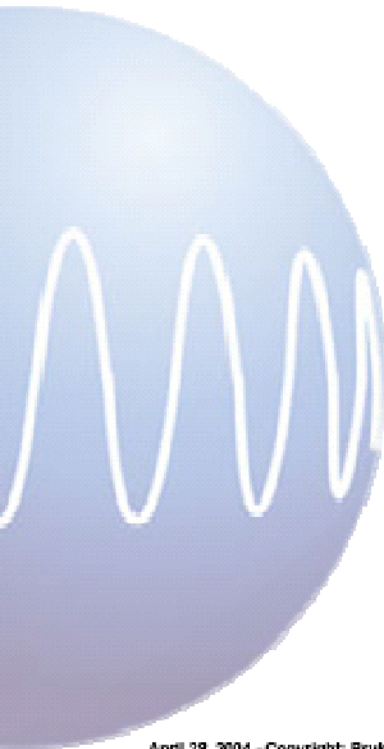


Fig.2: Distribution of the voxels within the language areas as function of the activation level.

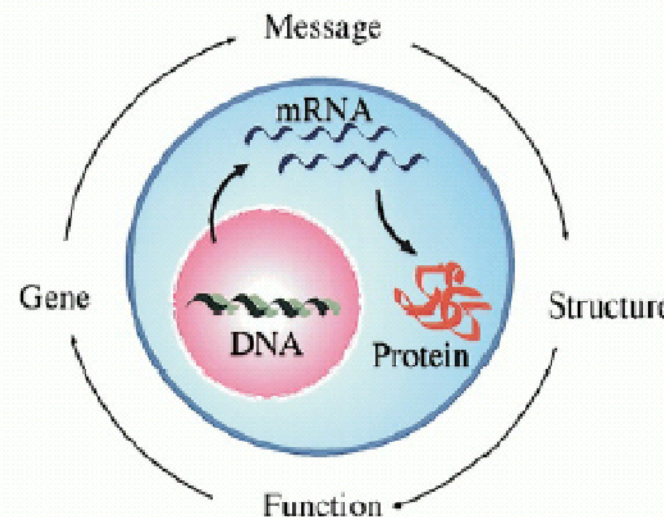
**antiepileptic drug topiramate (TPM) causes cognitive side effects. fMRI with word paradigm confirms this finding showing decreased activation especially in inferior (IPC) and medial prefrontal cortex (PFC)**

# MRI in Drug Development and Molecular Imaging



# Molecular Imaging Targets

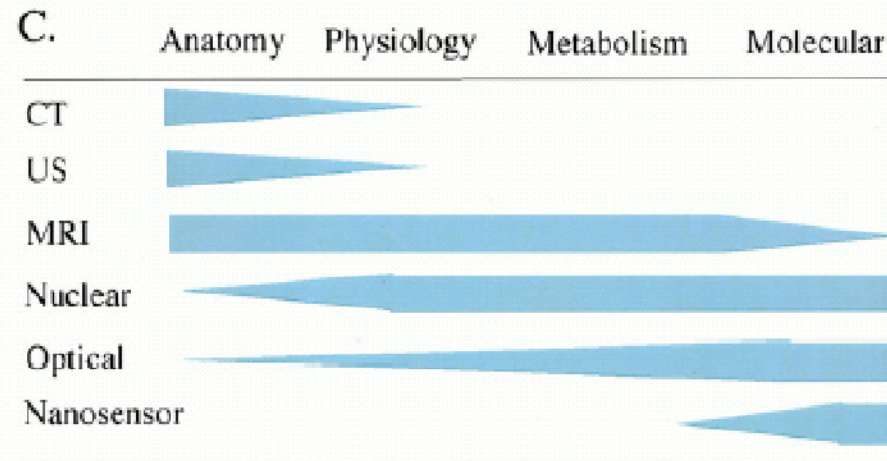
A.



Courtesy of  
 Piwnica-Worms,  
 Washington U., USA

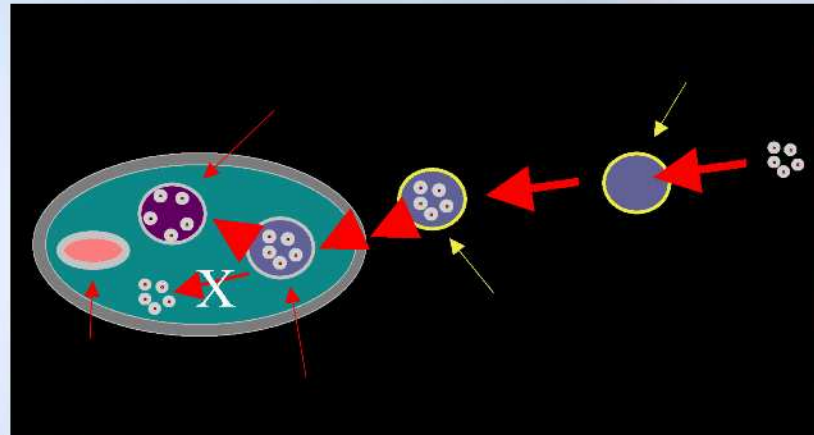
B.

Target	Number/cell
Gene (DNA)	2
Message	50-1,000
Protein	100 - 1,000,000
Function	massive

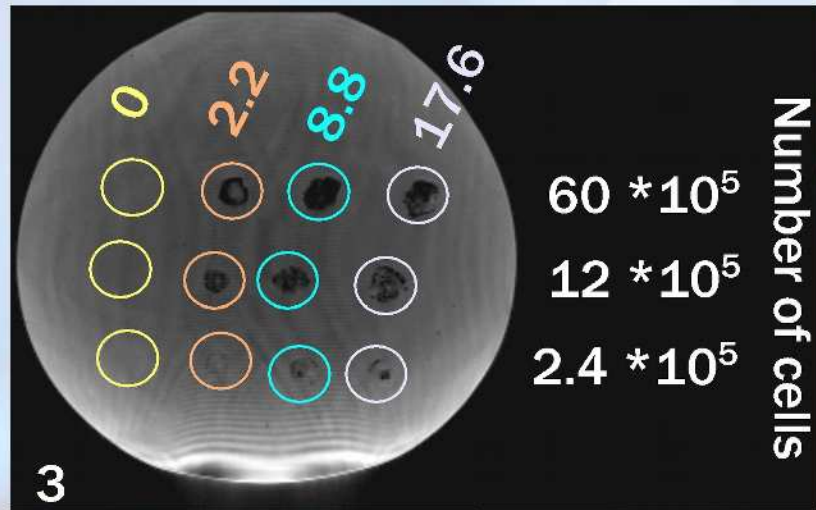


The schematic shows molecular imaging targets. A, Different intracellular imaging targets and their function are summarized. B, Numbers of targets per cell. C, Use of current imaging technology for molecular imaging: MRI covers almost the complete range and recently has been extended to the molecular level!

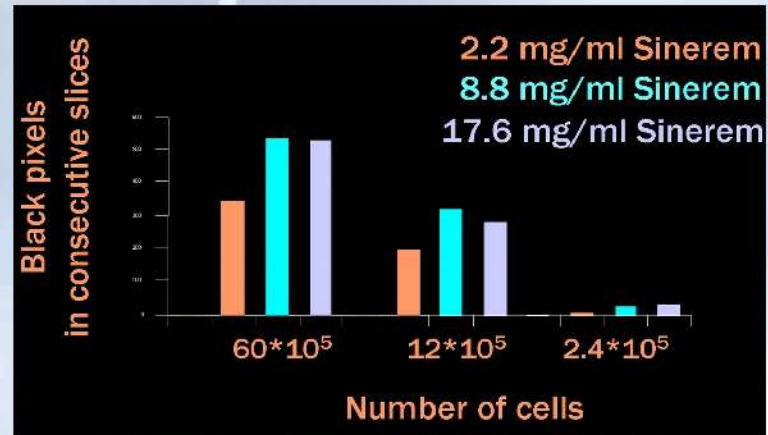
# (USPIO Labelling)



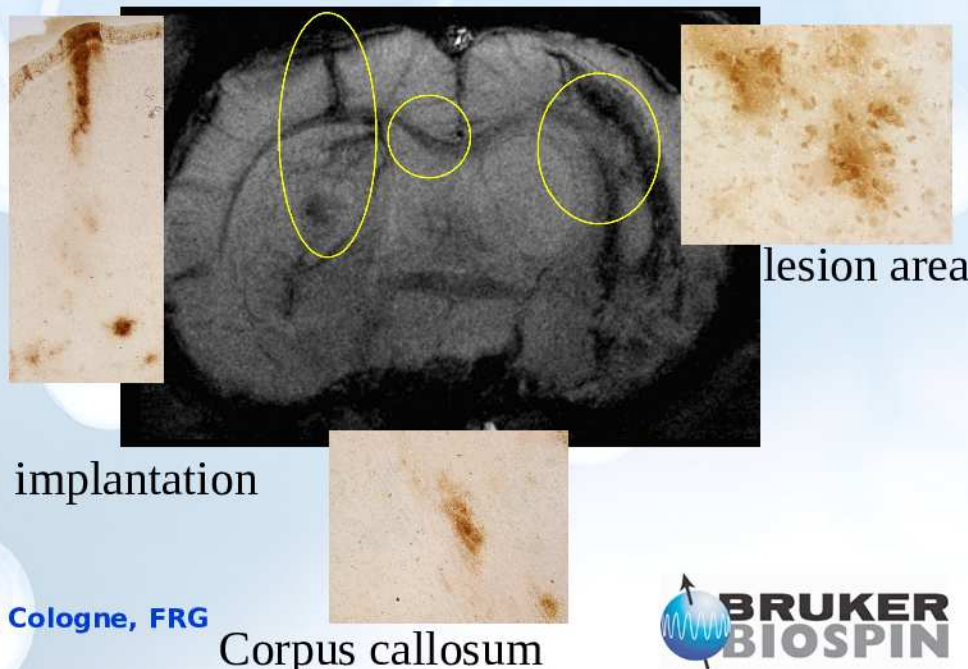
Loading of cells



saturation with iron oxide particles

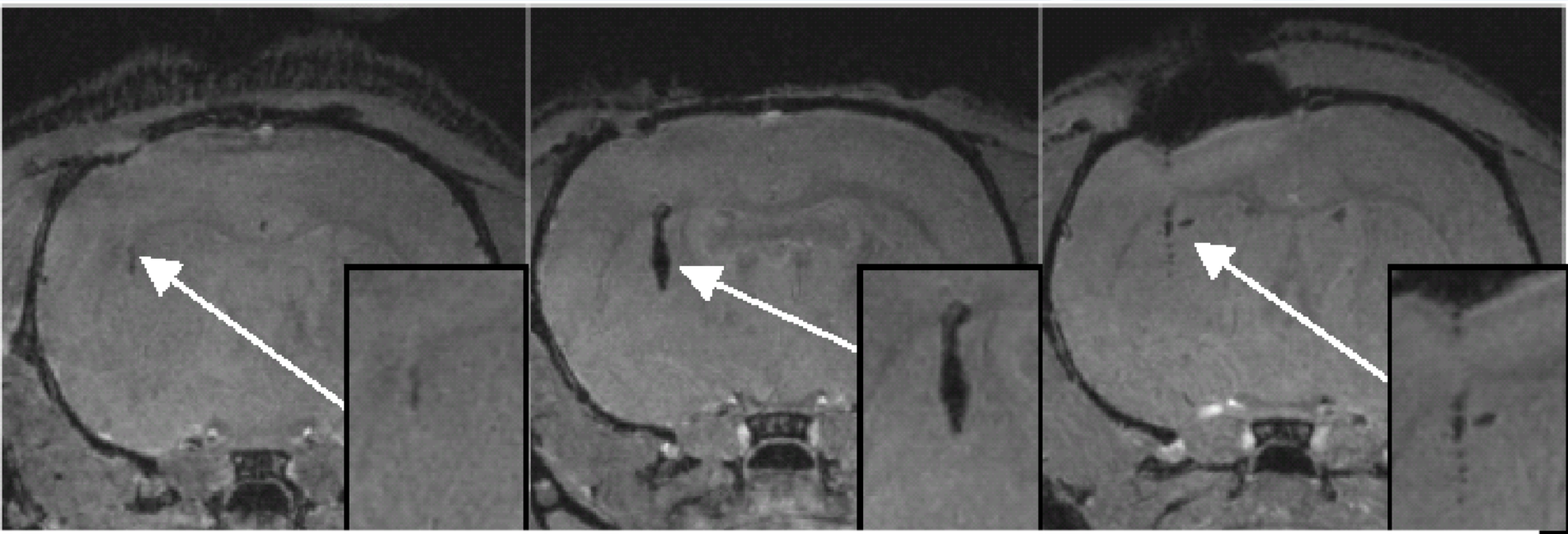


*Sinirem Concentration in subsequent slices*



# in vivo detection of a small amount of magnetically labeled stem cells

ISMRM 1737



Rat brain with different number of labeled cells

right: 1000 labeled cells      center: 10.000  
labelled cells                  left: 100 labeled cells

# Migration of stem cells in mouse brain

ISMRM 1744



Fig.1

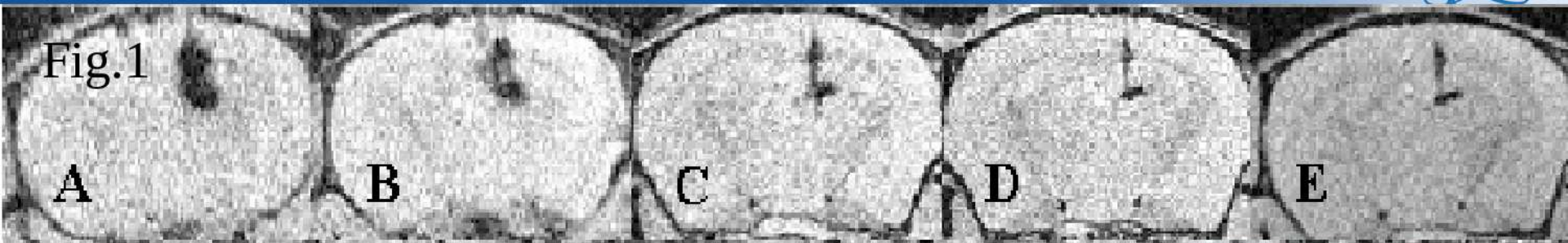


Fig.2

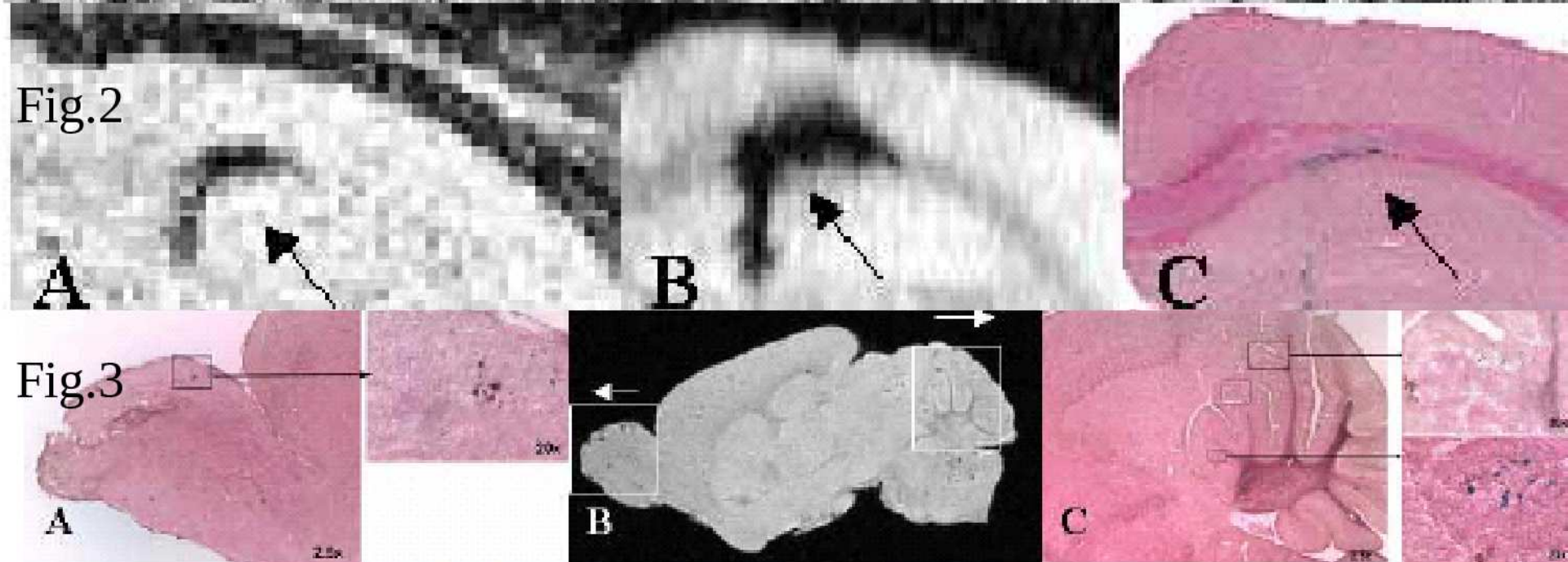
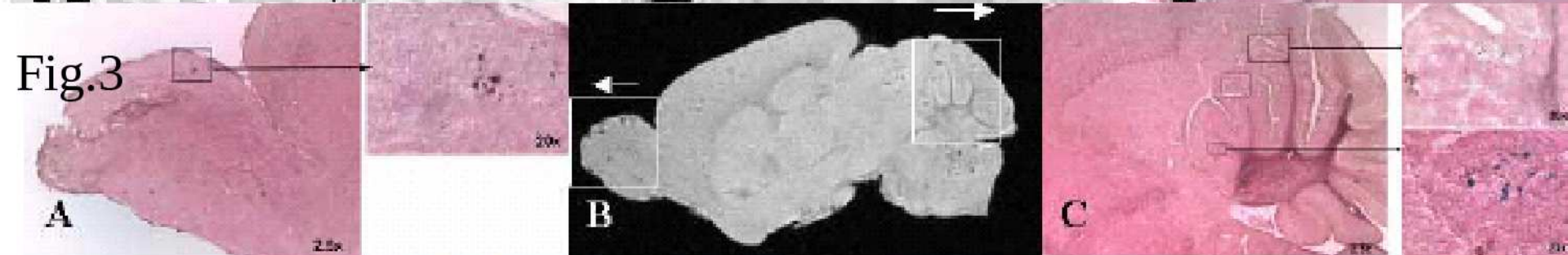


Fig.3



top: localization of injected stem cells after 1,7,16,21,32 days

center: conformation A:in vivo, B: ex vivo, C: Prussian blue staining

bottom: neonatal injection demonstrates broader distribution

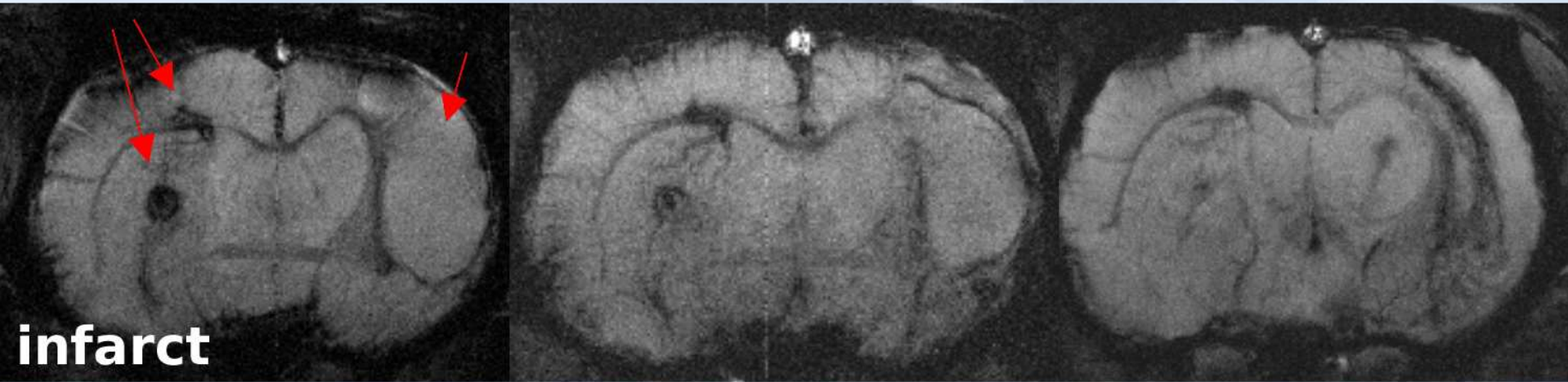
A,C:Prussian blue

B: area of MRU signal

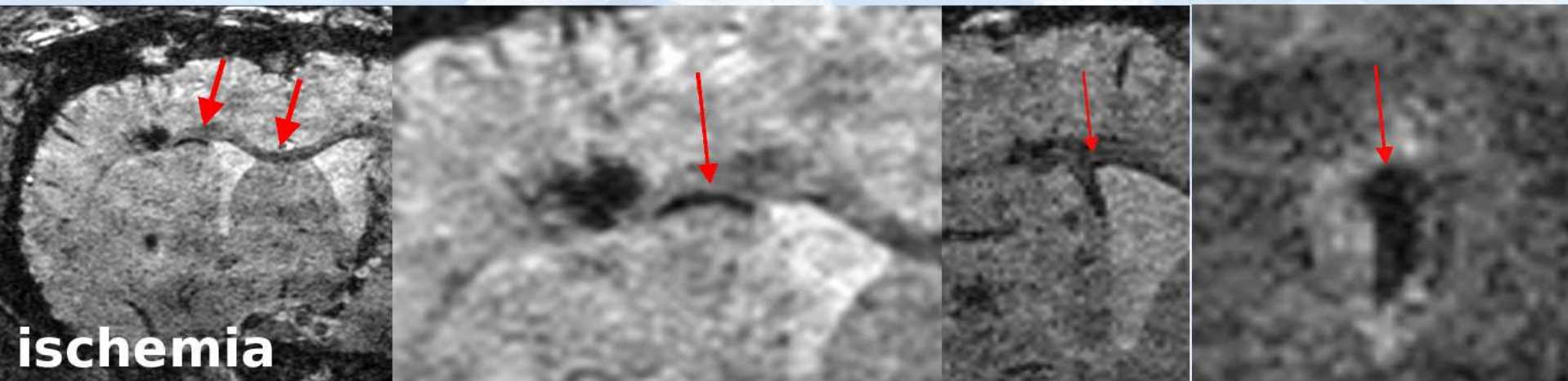
# Migration of stem cells



**USPIO-labeled embryonic stem cells migrate along corpus callosum to the lesion site**



infarct



ischemia

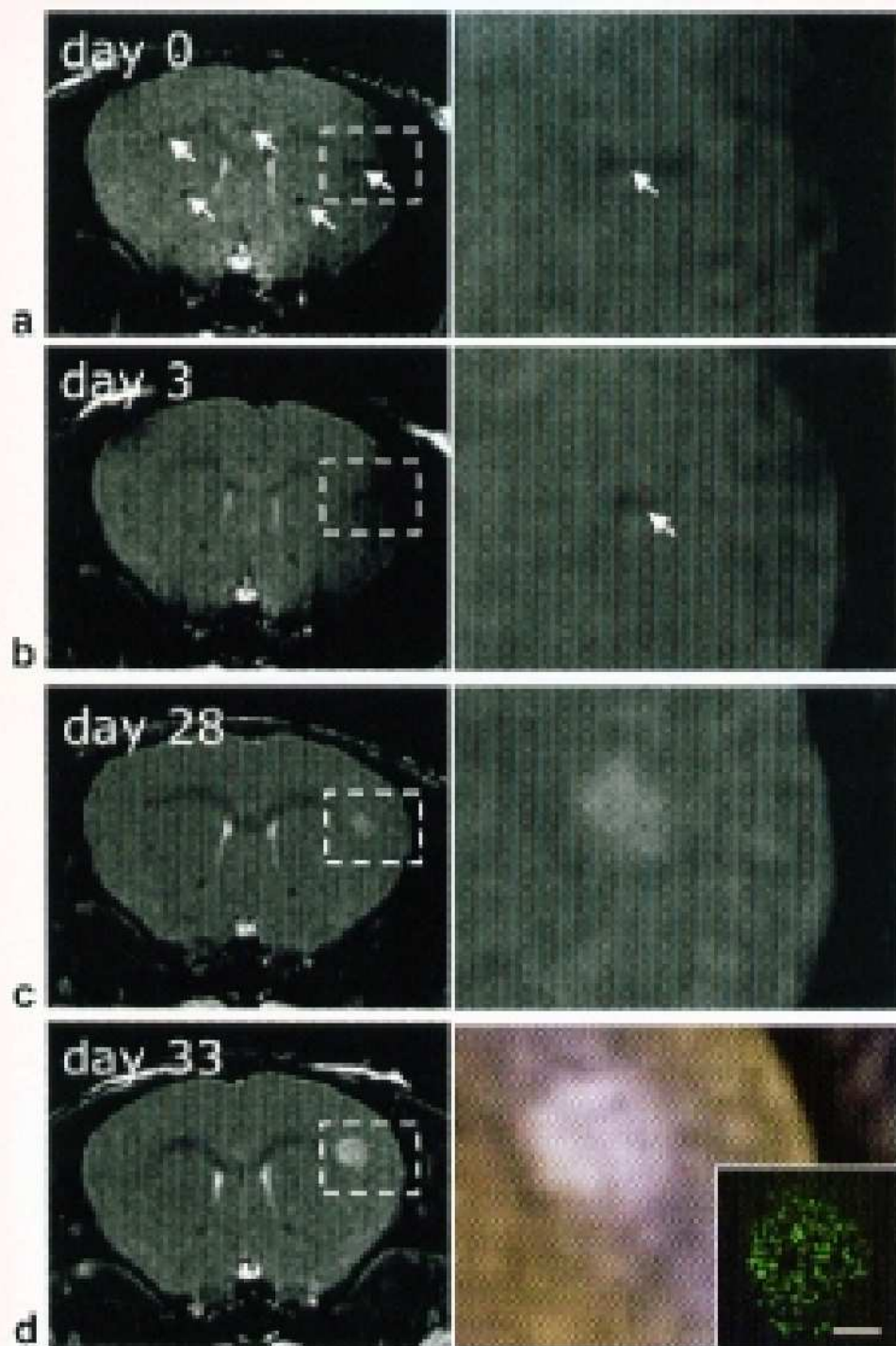
Courtesy of M. Höhn et al, Köln, Germany



# MRM 54(2006)1001

C.Heyn,J.A.Ronald,S.S.Ramadan,J.A.Snir,A.M.Barry,L.T.McKenzie,D.J.Mikulis,D.Palmieri,J.L.Bronder,P.S.Steeg,T.Yoneda,I.C.Mc.Donald,A.F.Chambers,B.K.Rutt,P.J.Foster

**In Vivo MRI of Cancer Cell Fate at the Single-Cell Level in a Mouse Model of Breast Cancer Metastasis to the Brain.**



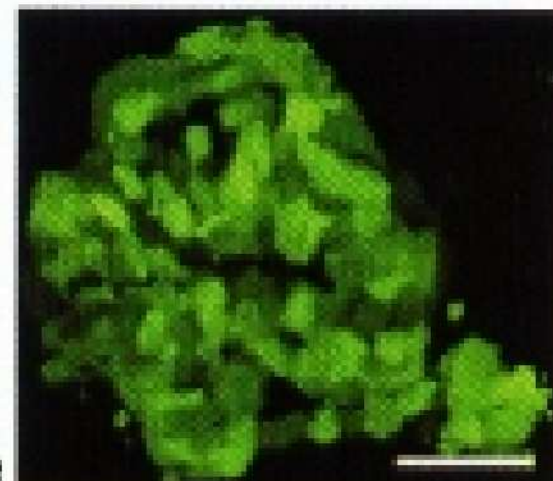
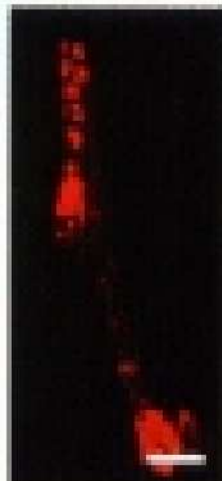
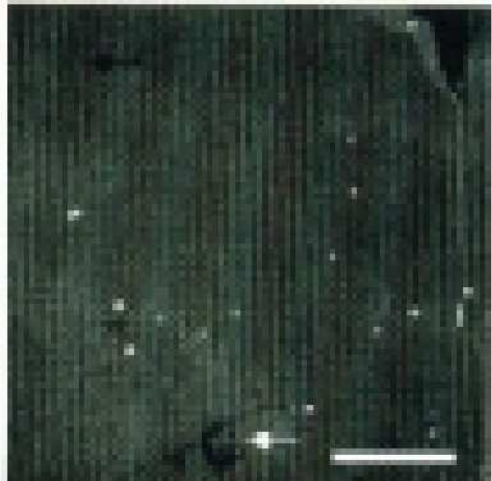
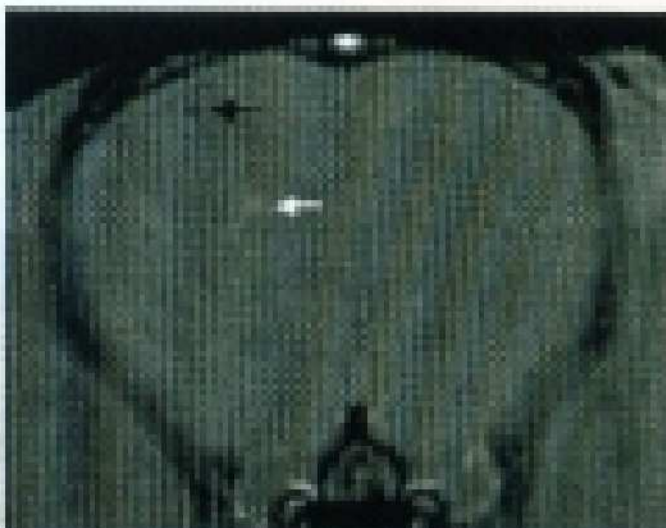
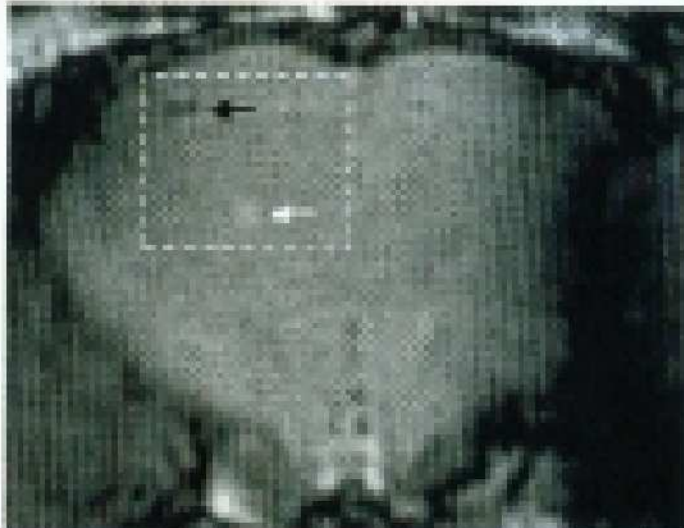
Tracking of growth of single labeled cell into a tumor.

- a. numerous signal voids at day 0
- b. on day 3 most signal voids have dissapeared, one remains
- c. area of hyperintensity at region of signal void on day 0-3
- d. hyperintense area has grown and confocal microscopy confirms a tumor

**in vivo**

**ex vivo**

**BRUKER**

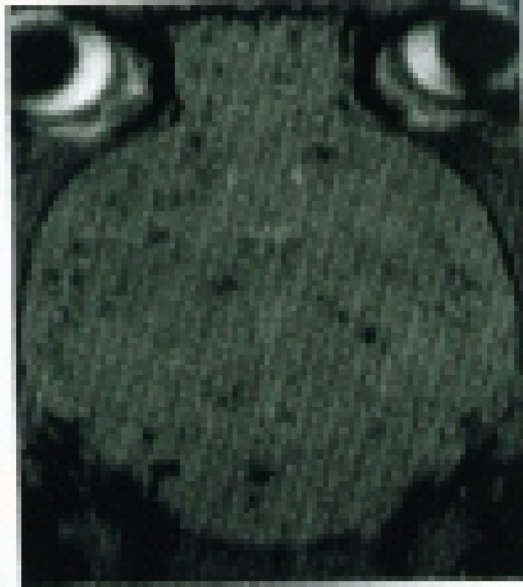


expansion of a.)

confocal microscopy

hyperintensity area: GFP+ tumor

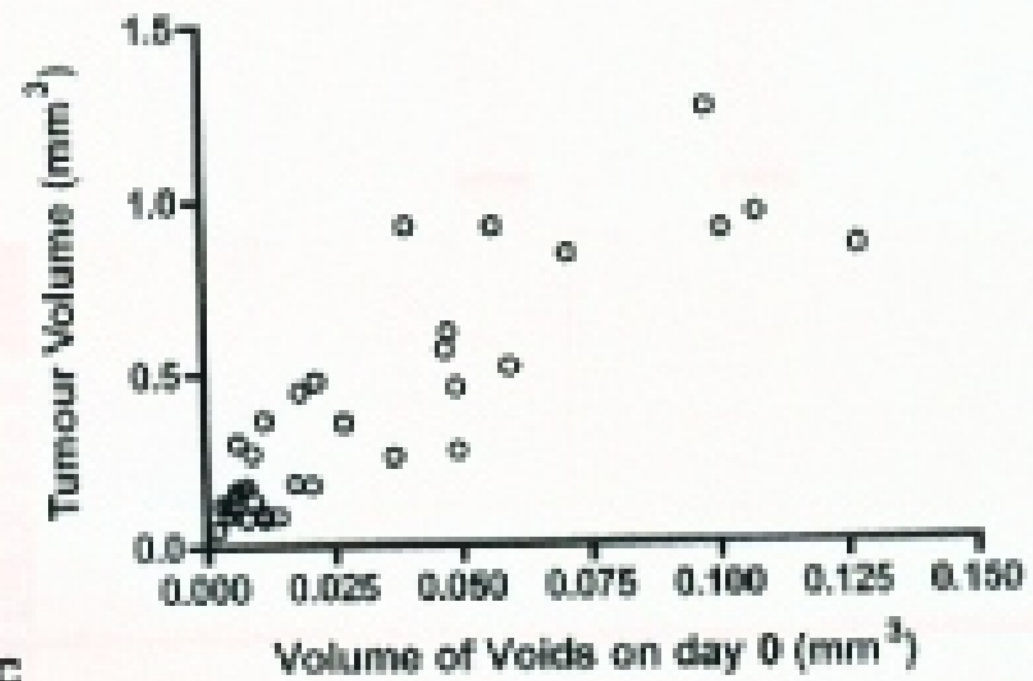
**BRUKER**  
**BIOSPIN**



a



b



c

a. Axial image after injection of 100.000 cell at day 0

The Bruker Biospin logo, featuring the word "BRUKER" in a bold, black, sans-serif font with a stylized blue and white swoosh graphic above it.

b. Cell fate map

blue areas correspond to transient tumor cells, which are visible on day 0 and disappear to day 28

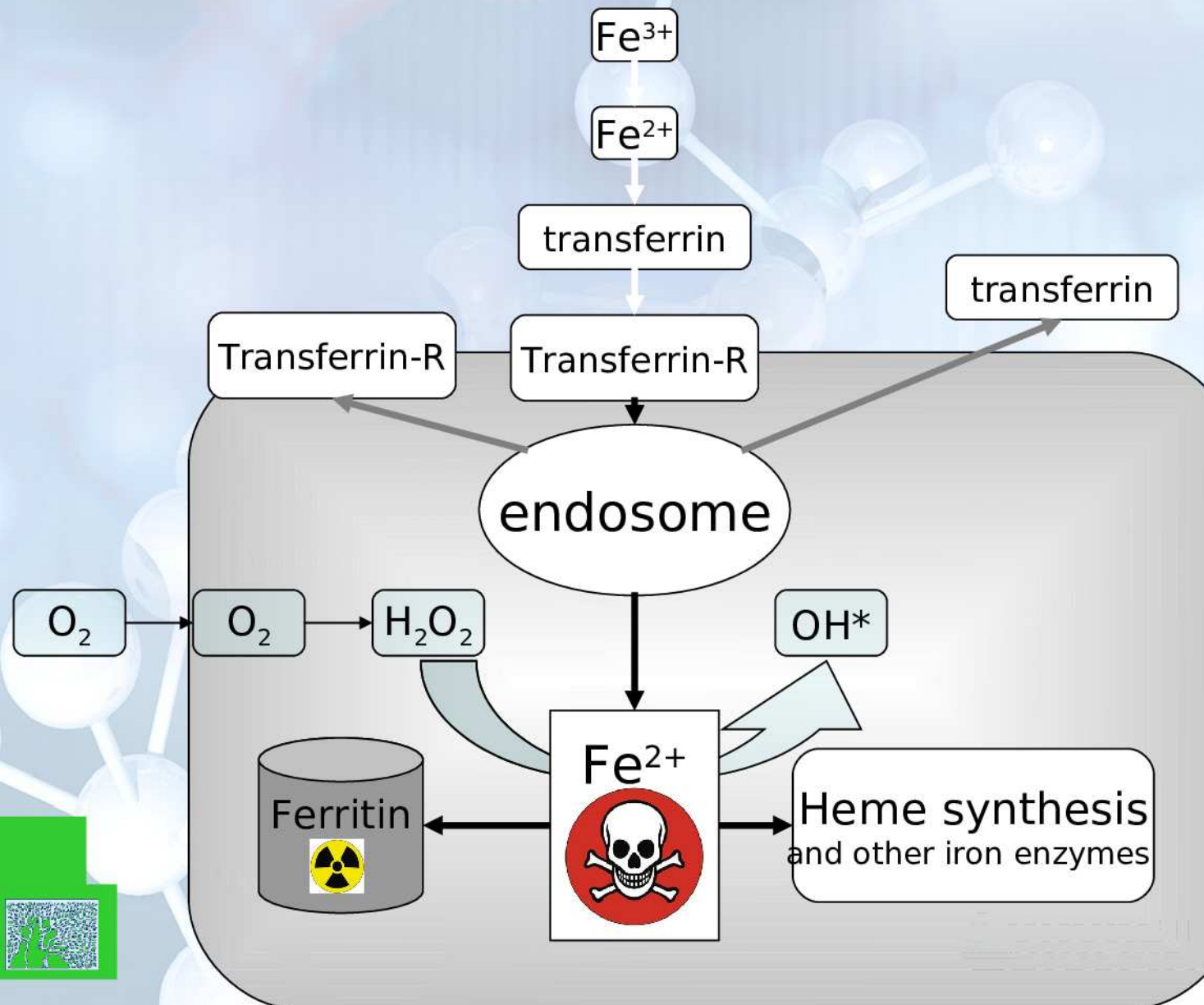
Green boundaries

correspond to tumors visible on day 28

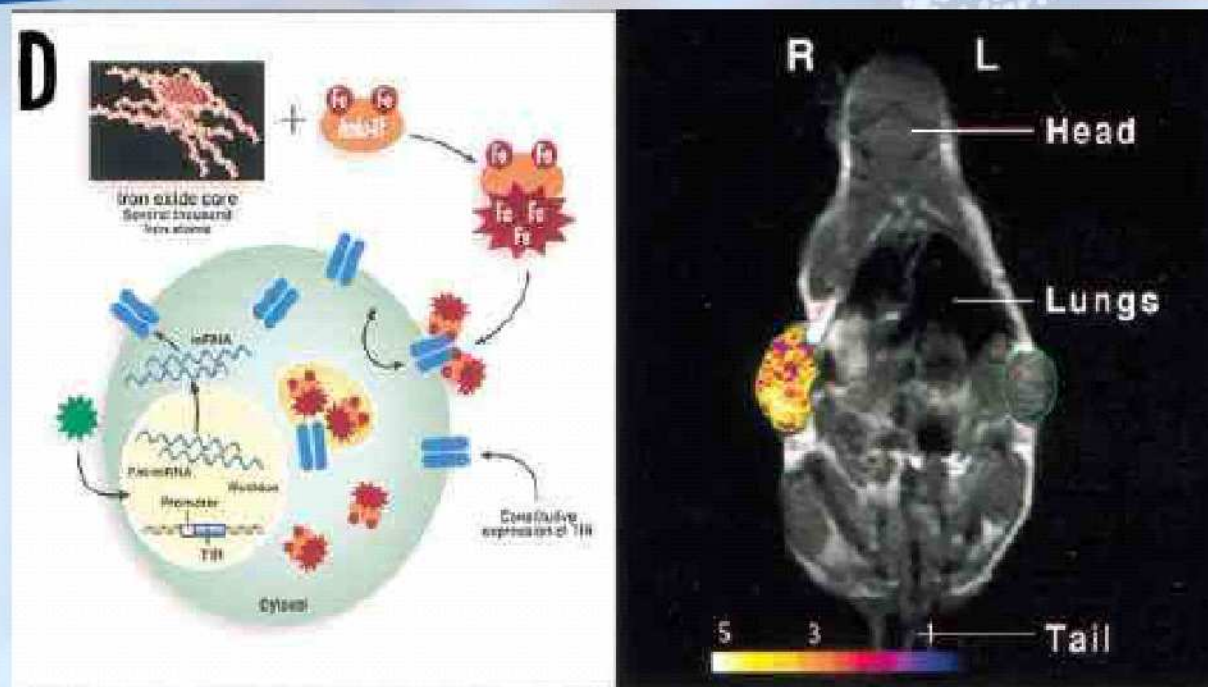
Red areas corresponds to cells, that give rise to tumors (proliferating tumor cells)

The Bruker Biospin logo, featuring the word "BRUKER" in a bold, black, sans-serif font with a stylized blue and white swoosh graphic above it.

# Ferritin as a reporter gene for MRI



# Receptor Based MRI MI

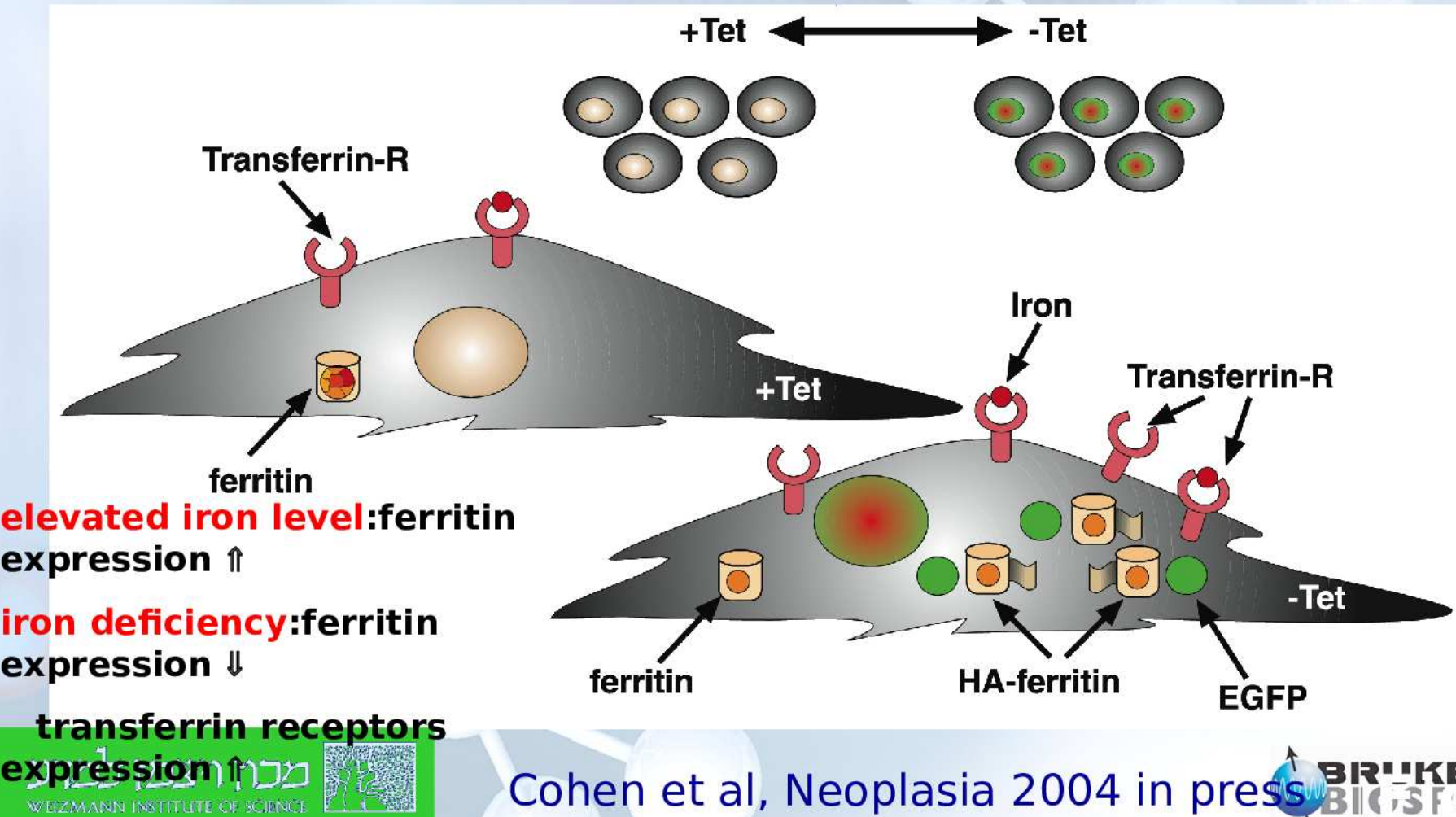


Courtesy of  
Weissleder, MGH,  
MA, USA

(D) Overexpression of engineered transferrin receptors (TfR) results in a ~500% increase in cell uptake of the transferrin-monocrystalline iron oxide nanoparticle (Tf-MION) probes. During each internalization event, several thousand iron atoms accumulate in the cytosol and within endosomes – without down-regulation of the level of receptor overexpression. These changes result in a detectable contrast change on MRI. The anatomical image is a T1-weighted spin echo image. Superimposed is a colored gradient echo MRI after Tf-MION administration, showing the increased uptake of iron only in the TfR<sup>+</sup> tumor (R). The TfR (L) tumor shows no uptake.

# Ferritin MR reporter for imaging gene expression

C6-pTET-EGFP-HA-ferritin tumors:  
Tetracycline inducible expression of EGFP and HA tagged ferritin.

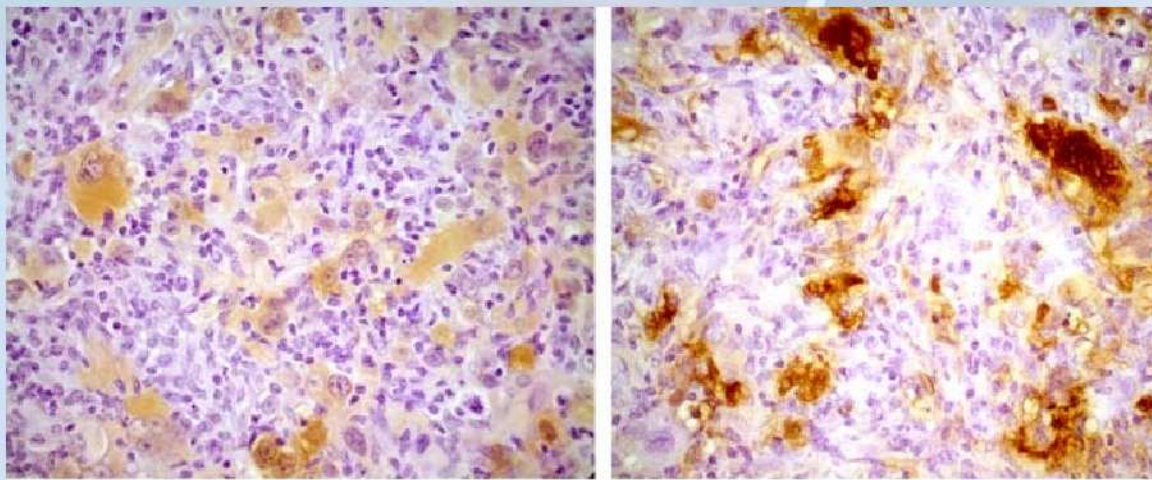


# Low EGFP-HA-ferritin

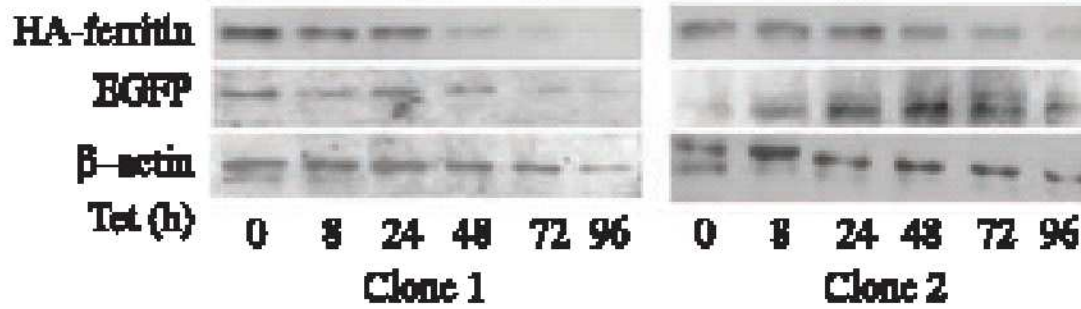
# High EGFP-HA-ferritin

BRUKER

EGFP



b



+Tet

-Tet

supression of EGFP and HA-ferritin by TET

מכון ויצמן למדע  
WEIZMANN INSTITUTE OF SCIENCE



BRUKER  
BIOSPIN

# Ferritin expression and intracellular iron content

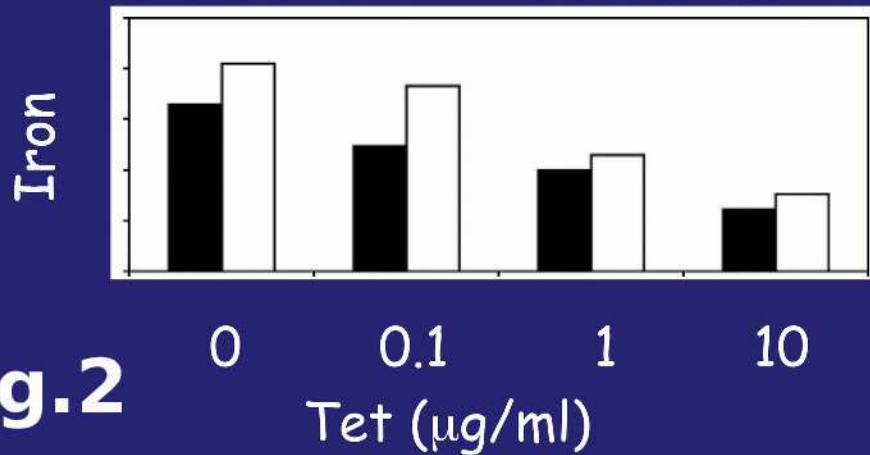


## Prussian Blue

Clone 1



Clone 2



supression of ferritin-overexpression by TET leads to iron-increase measured by prussian blue staining and ICP-AES

Clone 1 ■  
Clone 2 □

## ICP-AES

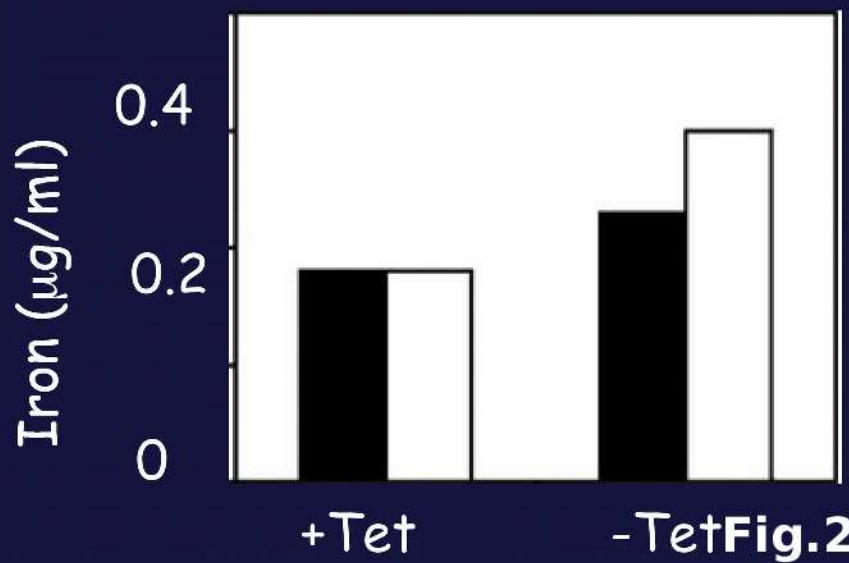


Fig.2

c

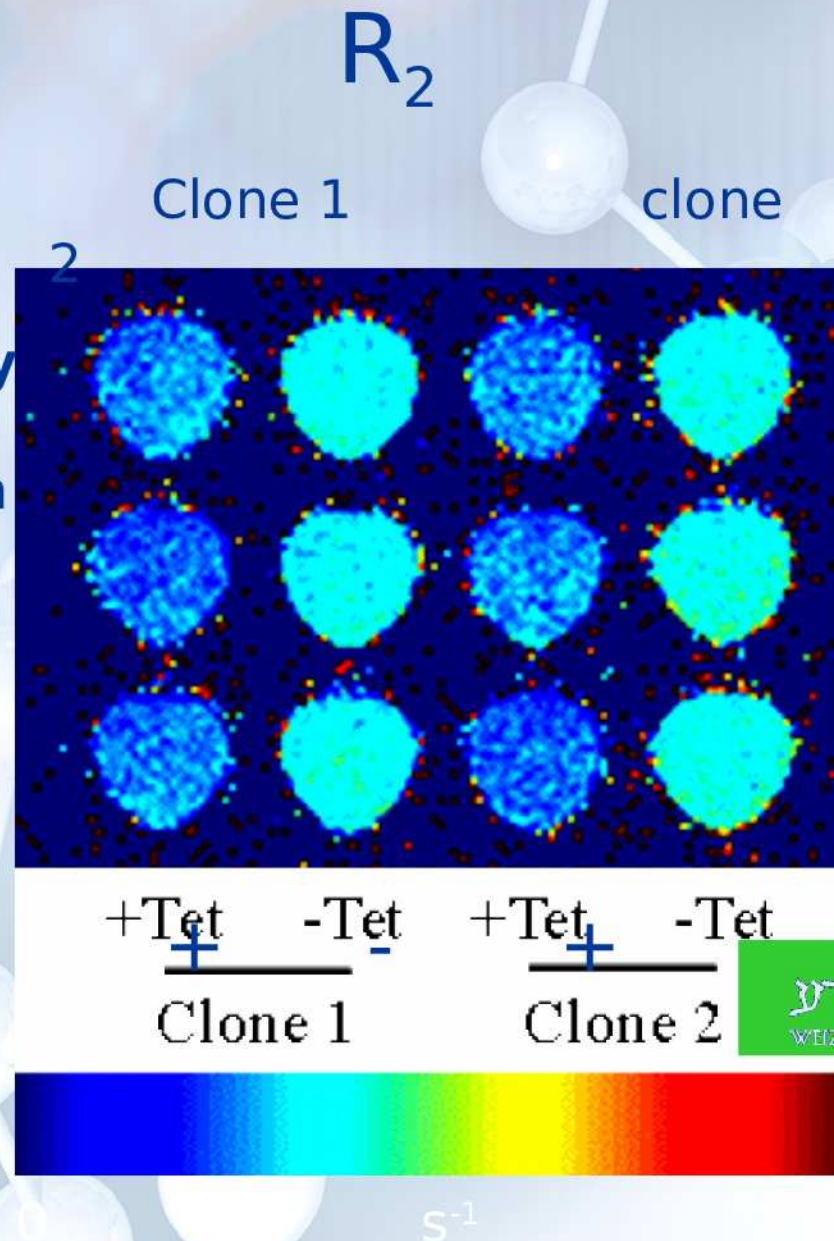


# **in vitro detection of ferritin expression in C6 rat glioma cells detected by relaxation rate R2**



**supression of  
ferritin-  
overexpression by  
TET leads to iron-  
increase resulting in  
reduced relaxivity  
R2**

**Tetracycline**  
-



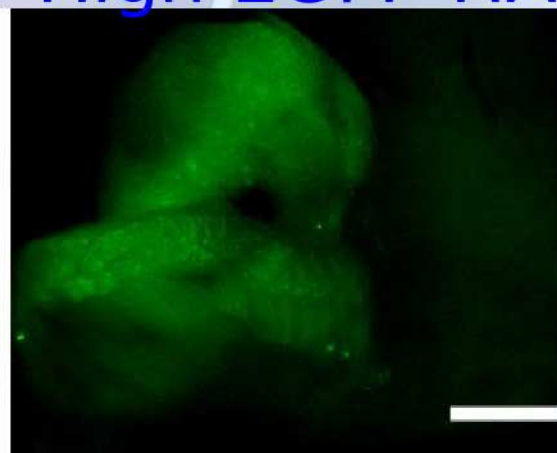
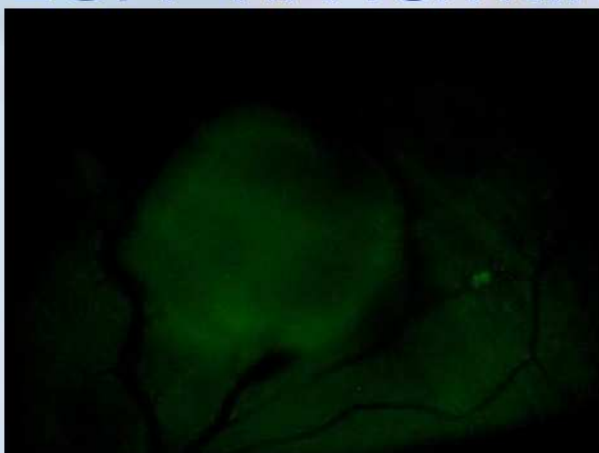
מכון ויצמן למדע  
WEIZMANN INSTITUTE OF SCIENCE



# MRI *in vivo* investigation of Ferritin overexpression

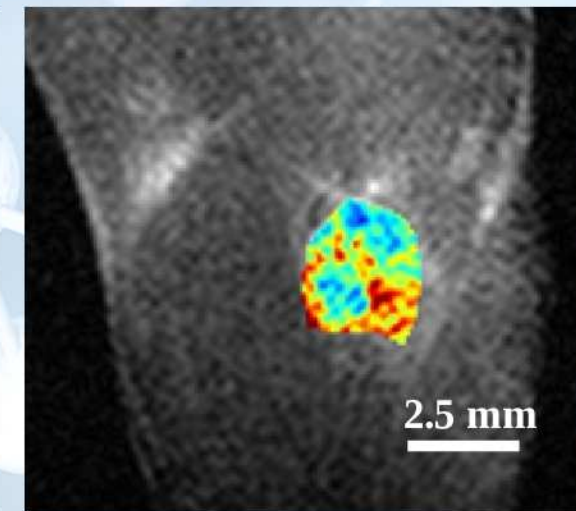
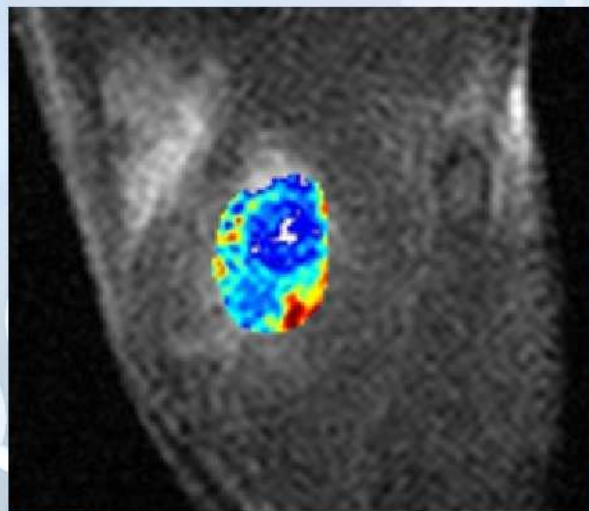


EGFP



expression of EGFP in subcutaneous tumors visualized by fluorescent microscopy

$R_2$



suppression of Ferritin overexpression by TET leads to increased MRI intensity due to higher  $R_2$  relaxation